ARKIV FÖR FYSIK Band 13 nr 38

Communicated 12 March 1958 by The Svedberg and Arne Westgren

Energy levels in Bi^{207} from the decay of Po^{207}

By E. Arbman, J. Burde[1] and T. R. Gerholm

With 11 figures in the text

ABSTRACT

The energy levels in Bi^{207} have been studied from the decay of 5.7 hr Po^{207}. The experiments include measurements of the energies and intensities of conversion electron lines and positron distributions in a double focusing spectrometer; measurements of gamma-ray spectrum in a scintillation spectrometer and to some extent in the double focusing spectrometer by the use of a lead converter; measurements of coincidences between pairs of conversion lines and between positrons and conversion lines in a double lens coincidence spectrometer, and coincidences between positrons and gamma rays in a beta-gamma coincidence spectrometer.

Two positron components of maximum energies 1140 keV and 893 keV were found, establishing the total decay energy of Po^{207} as 2.906 MeV. The proposed decay scheme contains 16 excited levels, 11 of which are considered to be well established. Spins and parities for the ground state of Po^{207} and the most strongly populated excited levels in Bi^{207} are given. The decay of Po^{207} is discussed on the basis of the shell model.

1. Introduction

The energy levels in nuclei in the neighbourhood of the double magic Pb^{208} nucleus are discussed from the standpoint of the single-particle shell model in a recent review article by Bergström and Andersson [1]. Low-lying levels can to a large extent be identified with single-particle levels. In cases where the nuclei differ by more than one nucleon from the Pb^{208} core, complex levels may arise due to coupling of the individual particles or holes to configurations in various ways. By the calculations of the levels in Pb^{206} and Pb^{205} on the basis of the shell model by Pryce [2, 3, 4] and recently in Pb^{206} by Kearsley [5] and by True and Ford [6] the main features of the complicated decays of Bi^{206} and Bi^{205} are explained. As Bi^{207} and Bi^{206} differ from Pb^{206} and Pb^{205} by the addition of one proton, an investigation of the levels in these nuclei seemed to be of interest. In this paper is described an investigation of the energy levels in Bi^{207} from the decay of Po^{207}. A calculation of the levels in Bi^{207} has been performed by Wahlborn [7], following the principles introduced by Pryce.

The 5.7 hr Po^{207} was identified by Templeton *et al.* [8] and was found to decay predominantly by electron capture to Bi^{207} and by a weak alpha branch ($\sim 0.01\,\%$)

---

[1] On leave from the Hebrew University, Jerusalem, Israel.

to Pb^{203}. Absorption analysis of the radiations emitted in the decay indicated gamma rays of energies about 1.3 MeV.

The electron capture decay of Po^{207} has recently been studied by Stoner [9]. Using permanent and variable field magnetic beta-ray spectrometers and scintillation spectrometers Stoner found transitions of energies 1148.5, 991.6, 742.8, 629.9, 405.5, 345.4, 329.1, 307, 270.8, 249.5, 233.0, 223.0 and 60.4 keV and transitions most probably present at energies of 177.5, 166.5, 135.5 and 124.0 keV. A number of weak conversion lines, which could not be assigned to definite transitions were observed in the electron spectrum obtained in the permanent magnet spectrograph. Furthermore the presence of positrons in the decay was proved by the annihilation radiation.

Gamma-gamma coincidences were measured by Stoner and the following results were observed: The 992 keV photopeak was found to be in coincidence with the 405, 743 and 1149 keV gamma rays; the 743 keV photopeak in coincidence with the 405 and 992 keV gamma rays; the 405 keV photopeak in coincidence with the 743 and 992 keV gamma rays and the 1149 keV peak in coincidence with the 992 keV gamma ray. Furthermore, by the investigation of coincidences with the K X-rays, using a fast coincidence unit, lifetime limits $\leqslant 5 \times 10^{-9}$ sec for the strong 405, 743 and 992 keV gamma rays could be set.

Based on the coincidence results obtained Stoner suggested a decay scheme with excited levels at 992, 1735, 2080, 2140 and 2362 keV. Several of the observed transitions could, however, not be placed in the suggested scheme.

In the present investigation about 40 transitions were found, including 10 of the transitions reported by Stoner. Conversion lines of the 270.8, 233.0, 60.4 and the probable 166.5, 135.5 and 124.0 keV transitions were not observed. Our proposed decay scheme differs entirely from that suggested by Stoner. The comparatively short half-life of Po^{207}, 5.7 hr, favoured the production of strong sources in the synchrocyclotron and thus enabled the investigation of weak transitions. On the other hand the short half-life was of disadvantage in particular for the time-consuming coincidence measurements.

In the following chapter the various measurements performed are reported. The decay scheme is discussed in chapter 3. In chapter 4 finally the decay of Po^{207} is discussed on the basis of the shell model.

2. Experimental procedures

2.1. *Instruments*

The excited levels in Bi^{207} were studied from the decay of 5.7 hr Po^{207}. Energies and relative intensities of the conversion electron lines and positrons emitted in the decay were measured in the double focusing spectrometer at the Gustaf Werner Institute [10]. In this spectrometer the coil current I can be accurately measured by compensation method and the $B\varrho$ value calculated from the formula $B\varrho = K(I) \times I$. $K(I)$ is determined by measuring conversion lines of known energies. Relative to appropriate chosen calibration lines the $B\varrho$ values can thus be accurately determined. The counter window used (~ 0.5 mg/cm^2 rubber hydrochloride) transmits electrons of energies higher than about 20 keV.

Relative gamma-ray intensities were deduced from the gamma-ray spectrum studied with a single channel pulse-height analyser [11] equipped with a 2.5 cm diameter, 2.5 cm high NaI(Tl) crystal. Relative gamma intensities were also obtained from a measurement in the double focusing spectrometer of the photoelectrons ejected in a lead converter.

The coincidence measurements were performed at the Physics Department of the University. Electron-electron and electron-positron coincidences were studied in the double lens coincidence spectrometer [12]. Measurement of coincidences between positrons and gamma rays was made in the beta-gamma coincidence spectrometer, provided with a 100-channel pulse analyser [13].

2.2. *Source preparation*

The Po^{207} activity was produced by bombarding bismuth with protons in the Uppsala synchrocyclotron through the $Bi^{209}(p,3n)Po^{207}$ reaction. Sources for the different kinds of spectrometers were prepared by electro-deposition of the polonium on silver-coated polythene or mylar films as previously described [14]. For the double focusing spectrometer sources with an area of about 1×15 mm² were used. Sources for the coincidence spectrometers and the scintillation spectrometer were prepared by plating the activity on circular silver spots of 2 or 3 mm diameter, evaporated onto a mylar backing of thickness 1.7 mg/cm².

According to the $Bi^{209}(p,xn)$ excitation curves by Bell and Skarsgard [15] the maximum yield of the $Bi^{209}(p,3n)Po^{207}$ reaction is obtained at about 30 MeV proton energy. Taking into account the energy spread (about 10 MeV at half maximum) of the internal proton beam of the synchrocyclotron [16], a somewhat higher maximum proton energy should be preferred in our case in order to produce Po^{207} in good yield. However, the simultaneous production of other polonium isotopes which may interfere in the measurements should be considered too. Intense conversion lines of short half-lives, probably due to the decay of Po^{205}, appeared at about 165 and 180 keV in a preliminary run of the conversion spectrum with a source prepared after an irradiation of bismuth by protons of 55 MeV energy. None of these lines were observed from a Po source, produced by 37 MeV maximum proton energy, which means that the yield of Po^{205} should be small at this bombarding energy. The 9 day Po^{206} lines, however, are comparatively strong (cf. Fig. 1). From the intensity of the conversion lines the Po^{206} activity was estimated to be about 1 % of the Po^{207} activity after a two hour bombardment at 37 MeV. In order to reduce further the yield of Po^{206}, which might interfere especially in the coincidence and scintillation spectrometer measurements, where comparatively poor resolution was obtained, most bombardments were performed at 34 MeV maximum proton energy.

2.3. *Conversion electron spectrum*

The conversion electron spectrum has been studied in the energy region 20 keV to 2.6 MeV. In Fig. 1 is shown a photograph of a record of the conversion lines from ~ 40 to 1100 keV, taken with the automatic device with a spectrometer resolution of 0.3 %. The decay of the lines was followed by taking records repeatedly. No line with a half-life which could not be ascribed to the decay of either the 5.7 hr Po^{207} or the 9 day Po^{206} was observed. To obtain more accurate intensity and energy values than was possible from the records, all lines were remeasured point by point. In the energy region below about 1100 keV the measurements were performed with a momentum resolution of about 0.2 %. The weak lines at higher energies were studied at about 0.45 % resolution.

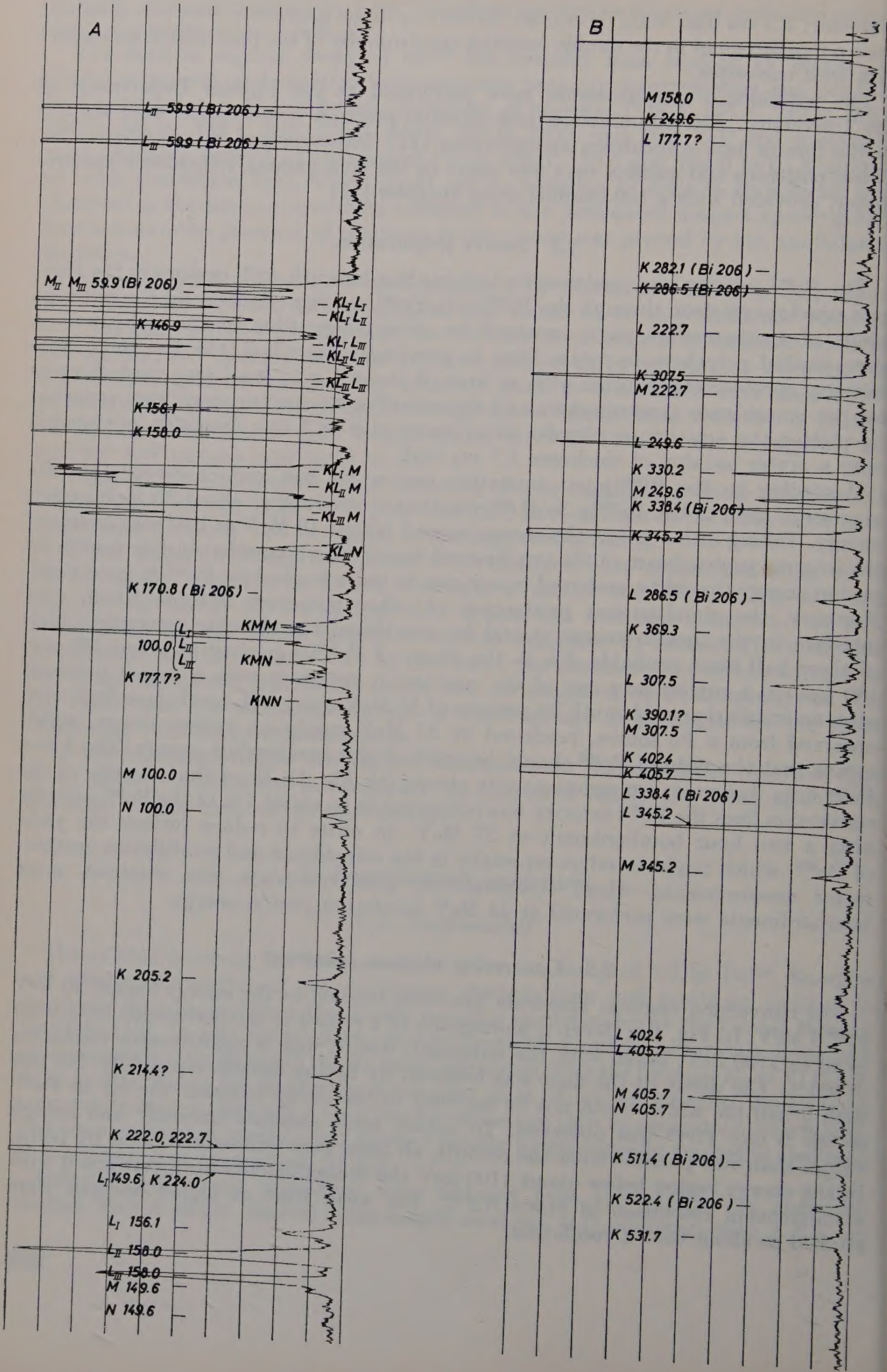
A
L_{II} 59.9 (Bi 206)
L_{III} 59.9 (Bi 206)
M_{II} M_{III} 59.9 (Bi 206)
$KL_{I}L_{I}$
$KL_{I}L_{II}$
K 146.9
$KL_{I}L_{III}$
$KL_{II}L_{III}$
$KL_{III}L_{III}$
K 156.1
K 158.0
$KL_{I}M$
$KL_{II}M$
$KL_{III}M$
$KL_{III}N$
K 170.8 (Bi 206)
100.0 L_{I} L_{II} L_{III}
KMM
KMN
K 177.7?
KNN
M 100.0
N 100.0
K 205.2
K 214.4?
K 222.0, 222.7
L_{I} 149.6, K 224.0
L_{I} 156.1
L_{II} 158.0
L_{III} 158.0
M 149.6
N 149.6
B
M 158.0
K 249.6
L 177.7?
K 282.1 (Bi 206)
K 286.5 (Bi 206)
L 222.7
K 307.5
M 222.7
L 249.6
K 330.2
M 249.6
K 338.4 (Bi 206)
K 345.2
L 286.5 (Bi 206)
K 369.3
L 307.5
K 390.1?
M 307.5
K 402.4
K 405.7
L 338.4 (Bi 206)
L 345.2
M 345.2
L 402.4
L 405.7
M 405.7
N 405.7
K 511.4 (Bi 206)
K 522.4 (Bi 206)
K 531.7

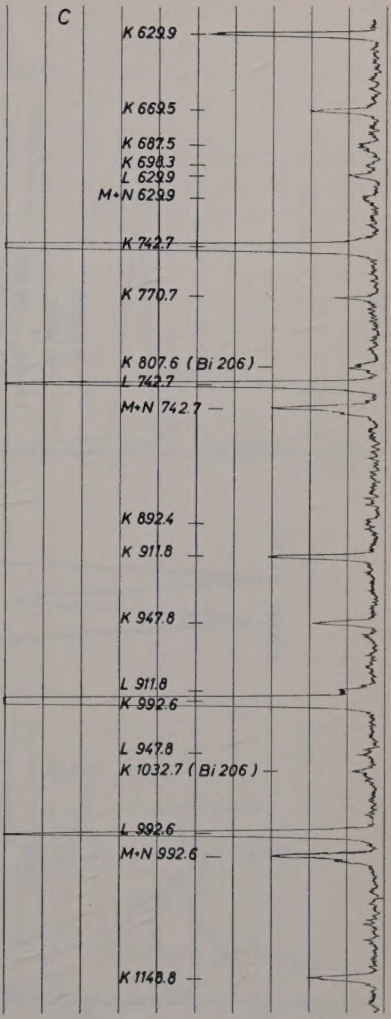

Fig. 1. Photographs of the conversion electron spectrum recorded in the double focusing spectrometer with the aid of the automatic device. The source prepared after a bombardment of Bi with protons of 37 MeV maximum energy. Energy ranges: (A) 40 keV to 145 keV; (B) 145 keV to 500 keV; (C) 530 keV to 1100 keV. Spectrometer resolution 0.3 %. Full scale deflection 100 counts/sec.

The energy region from 1 to 2.6 MeV was carefully investigated using strong sources in order to find possible weak cross-over transitions, which might be of importance in constructing the decay scheme. Part of the high energy spectrum is shown in Fig. 2. Above the conversion lines of the 2061 keV transition no line was found up to the energy of 2.6 MeV. From the measurements it is estimated that a possible conversion line with an intensity $\geqslant \frac{1}{20}$ of the intensity of the 2061 keV K line would have been observed.

The strong K conversion lines of the 286.5, 338.4, 511.4, 807.6 and 1032.7 keV transitions in Bi^{206}, always present in the sources under investigation, were used as reference lines for energy calibration of the spectrometer. The energies of these lines have previously been accurately determined [14]. At low energies the calibra-

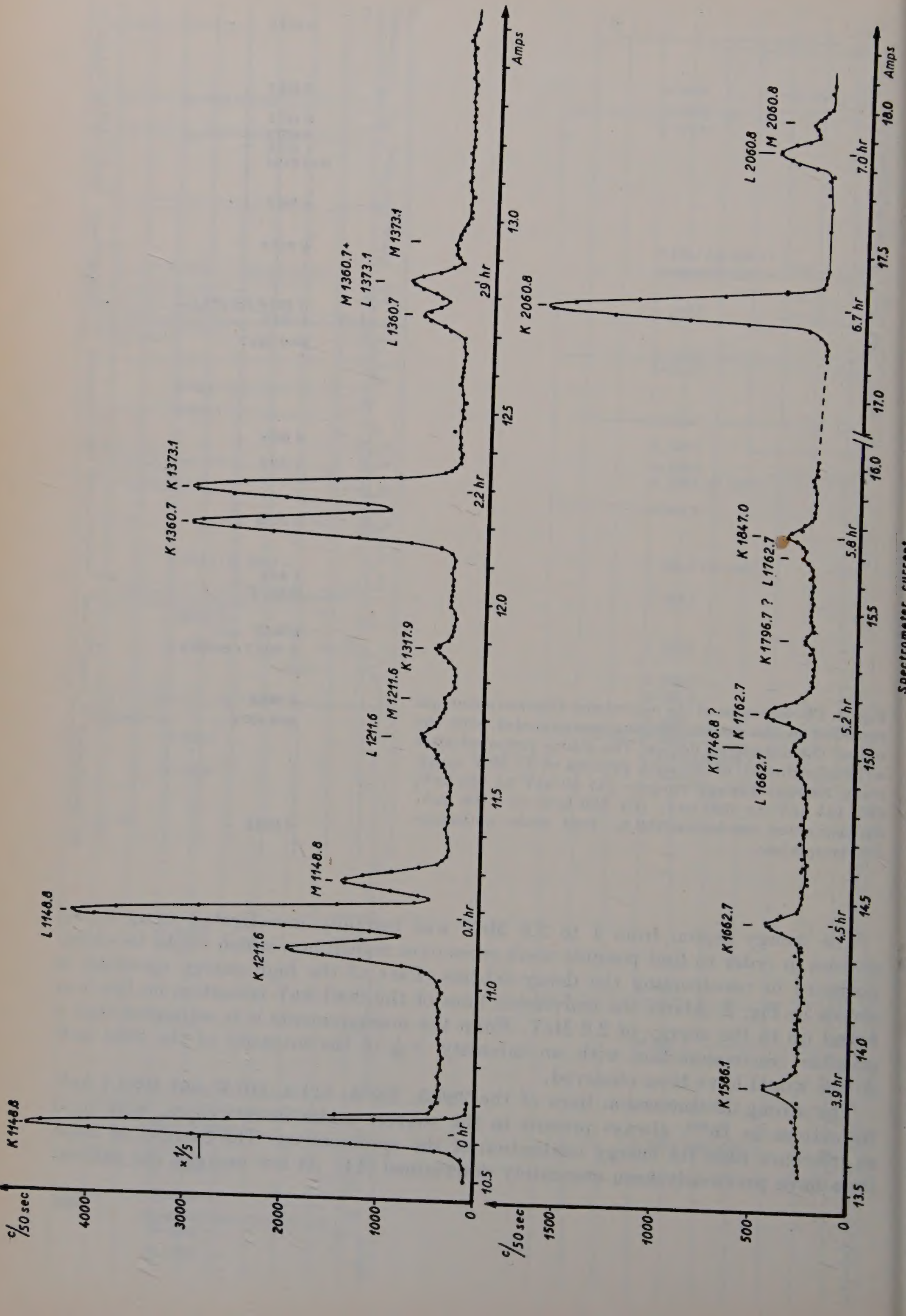
c/50 sec
4000
3000
2000
1000
0
K 1148.8
x 1/5
0 hr
K 1211.6
L 1148.8
0.7 hr
M 1148.8
L 1211.6
M 1211.6
K 1317.9
K 1360.7
K 1373.1
2.2 hr
L 1360.7
L 1373.1
M 1360.7+
M 1373.1
2.9 hr
Amps
10.5
11.0
11.5
12.0
12.5
13.0
c/50 sec
1500
1000
500
0
K 1586.1
3.9 hr
K 1662.7
4.5 hr
L 1662.7
K 1746.8 ?
K 1762.7
5.2 hr
K 1796.7 ?
L 1762.7
K 1847.0
5.8 hr
K 2060.8
6.7 hr
L 2060.8
M 2060.8
7.0 hr
13.5
14.0
14.5
15.0
15.5
16.0
17.0
17.5
18.0
Amps
Spectrometer current

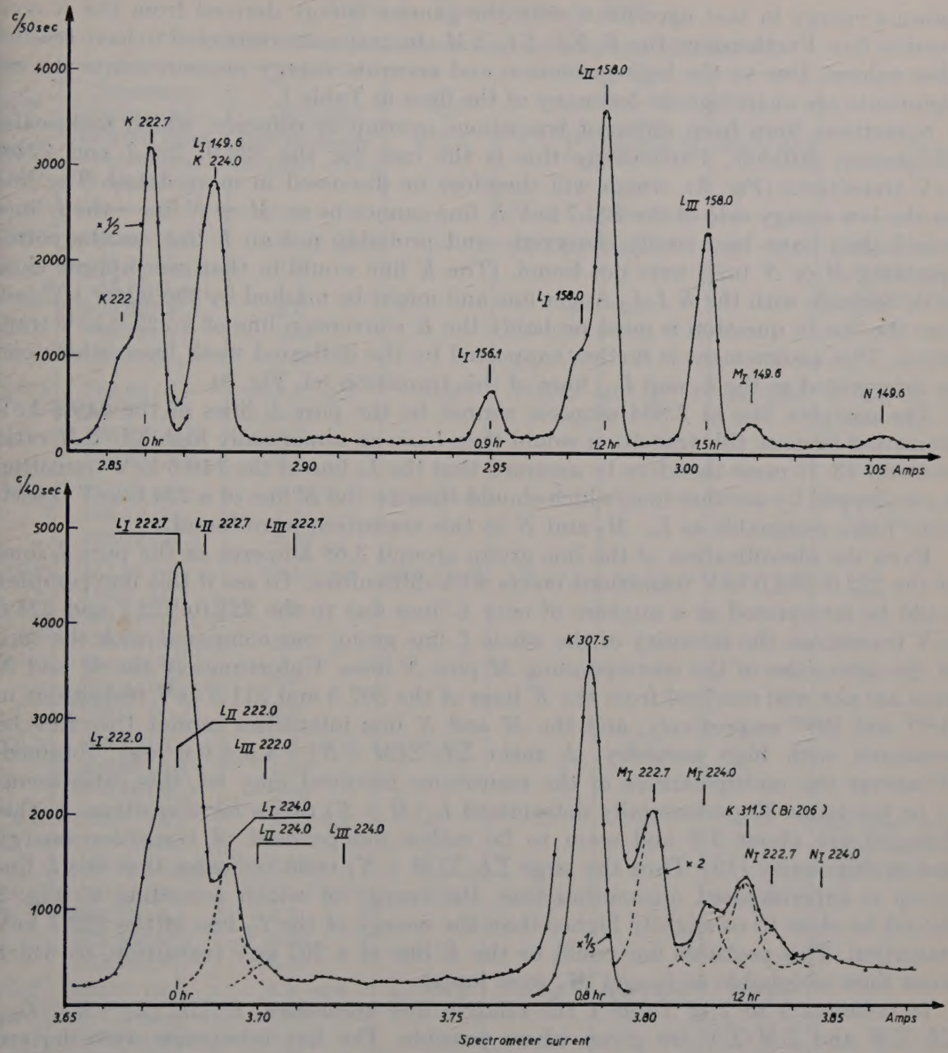

Fig. 3. Conversion lines of the 222.0–224.0 keV transitions. The K and L lines are measured using different sources with a resolution of about 0.2 %.

tion of the spectrometer was checked against the $KL_{\mathrm{III}}L_{\mathrm{III}}$ Auger line, the energy of which has been determined with an accuracy of 0.03 % by Mladjenović and Slätis [17].

The conversion lines observed from the decay of Po^{207} are listed in Tables 1 and 2. Table 1 contains all those lines whose transition assignments are believed to be certain. The binding energies in various shells of electrons used in calculating the gamma energies are taken from the table given by Hill *et al.* [18]. The line assignment L_{I}, L_{II} ... etc. for a definite transition is made according to which assignment gives a gamma energy in best agreement with the gamma energy derived from the K conversion line. Furthermore the $K/\Sigma L$, $\Sigma L/\Sigma M$ etc. ratios are restricted to have reasonable values. Due to the high resolution and accurate energy measurements the assignments are unambiguous for many of the lines in Table 1.

Sometimes lines from different transitions overlap or coincide, which makes the assignment difficult. Particularly this is the case for the 222.0, 222.7 and 224.0 keV transitions (Fig. 3), which will therefore be discussed in more detail. The line on the low energy side of the 222.7 keV K line cannot be an M or N line—the L lines would then have been easily observed—and probably not an L line, as the corresponding M or N lines were not found. (The K line would in that case appear close to or coincide with the $K\,L_IL_I$ Auger line and might be masked by the latter.) Therefore the line in question is most probably the K conversion line of a 222.0 keV transition. This assignement is further supported by the indicated weak lines, which can be interpreted as the L_I and L_{III} lines of this transition (cf. Fig. 3).

The complex line at 2.864 amperes cannot be the pure L lines of the 149.6 keV transition because this transition would then have an abnormally high $\Sigma L/\Sigma M$ ratio of about 13. It must therefore be assumed that the L_I line of the 149.6 keV transition is overlapped by another line, which should then be the K line of a 224.0 keV transition. Lines assignable as L_I, M_I and N to this transition were found.

Even the identification of the line group around 3.68 amperes as the pure L lines of the 222.0–224.0 keV transitions meets with difficulties. To see if this line complex could be interpreted as a mixture of only L lines due to the 222.0, 222.7 and 224.0 keV transitions the intensity of the whole L line group was compared with the sum of the intensities of the corresponding M plus N lines. Unfortunately the M and N lines are not well resolved from the K lines of the 307.5 and 311.5 keV transitions in Bi^{207} and Bi^{206} respectively, and the M and N line intensities cannot therefore be measured with high accuracy. A ratio $\Sigma L/\Sigma(M+N) = 4.5 \pm 0.6$ was obtained. Whatever the multipolarities of the transitions involved may be, this ratio seems to be too large. Experimentally determined $L/(M+N)$ ratios for transitions in this Z-region are about 3.2 and seem to be rather independent of transition energy and multipolarity [19]. Thus the large $\Sigma L/\Sigma(M+N)$ ratio indicates that the L line group is superimposed on another line, the energy of which according to Fig. 3 should be close to or slightly higher than the energy of the L_I line of the 222.7 keV transition. This probable line could be the K line of a 297 keV transition, to which weak lines assignable as L_I and M_I were found.

In columns 3 to 7 of Table 1 the relative line intensities, $K/\Sigma L$, $(L_I + L_{II})/L_{III}$, $\Sigma L/\Sigma M$ and $\Sigma M/\Sigma N$ are given where possible. The line intensities were derived from the measured areas of the conversion lines. It should be noted that the $K/\Sigma L$ ratios in several cases are determined more accurately than the overall relative line intensities. In some transitions the L lines were masked by other lines, while the intensities of the M lines could be measured. In order to get approximate $K/\Sigma L$ ratios in these cases, e.g. for the transitions of energies 149.6, 222.7, 330.2 and 669.5 keV, the L line intensities were estimated using the relation $\Sigma L/\Sigma M = 4$. The $K/\Sigma L$ and $\Sigma L/\Sigma M$ ratios derived with this assumption are placed within parentheses in Table 1. From the $K/\Sigma L$ and $(L_I + L_{II})/L_{III}$ ratios multipolarities of the gamma rays may be assigned. This is further discussed in section 2.4.

Table 2 contains conversion lines for which definite assignments were not possible. Many of these lines are very weak and are only slightly indicated in the conversion electron spectrum. As the half-life for the weakest lines could not be followed all

Table 1. Transitions in Bi^{207}.

Values within parentheses deduced assuming $\Sigma L/\Sigma M = 4$.

dopted nsition nergy keV)	Transition energy calculated from conversion lines (keV)	Relative line intensity (K 405.7 = 100)	$K/\Sigma L$	$(L_{\rm I}+L_{\rm II})/L_{\rm III}$	$\Sigma L/\Sigma M$	$M/(N+O)$	Remarks
.0 ± 0.1	99.96 ($L_{\rm I}$) 99.95 ($L_{\rm II}$) 99.97 ($L_{\rm III}$) 100.03 ($M_{\rm I}$) 99.99 ($N_{\rm I}$) 99.97 ($O_{\rm I}$)	9.8 ± 1.0 1.7 1.4 3.0 0.60 0.22	—	8.2 ± 1.2	4.3 ± 0.4	3.7 ± 0.7	L lines composite with KMM and KMN Auger lines
.6 ± 0.1	149.65 (K) 149.6 ($L_{\rm I}$) 149.62 ($M_{\rm I}$) 149.60 ($N_{\rm I}$)	12.0 ± 1.5 (2.3) 0.58 0.2	(5.2)	(⩾16)	(4)	3.0 ± 0.6	K and $L_{\rm I}$ lines composite with the $KL_{\rm II}L_{\rm II}$ and the 224 keV K lines respectively
.1 ± 0.1	156.08 (K) 156.11 ($L_{\rm I}$) 156.12 ($M_{\rm I}$)	7.2 ± 0.7 1.2 0.32	5.8 ± 0.6	—	3.9 ± 0.6	—	Possible $L_{\rm III}$ line hidden by 158.0 keV $L_{\rm II}$ line
.0 ± 0.1	157.97 (K) 158.0 ($L_{\rm I}$) 158.01 ($L_{\rm II}$) 158.04 ($L_{\rm III}$) 158.05 ($M_{\rm II}$) 158.04 ($M_{\rm III}$) 158.0 $N_{\rm II}$)	11.5 ± 1.0 9.9 5.3 4.5 1.5	0.75 ± 0.08	1.9 ± 0.2	3.4 ± 0.6	3.0 ± 0.6	
.2 ± 0.2	205.27 (K) 205.22 ($L_{\rm I}$) 205.16 ($M_{\rm I}$)	1.2 ± 0.2 0.23 ~0.05	5.1 ± 0.7	—	4 ± 1	—	
.0 ± 0.3	222.0 (K) ≈222 ($L_{\rm I}$) 222.1 ($L_{\rm III}$)	3.5 ± 0.8 ~0.15	—	—	—	—	All lines interfere with the lines of the 222.7 keV transition
.7 ± 0.2	222.71 (K) 222.75 ($L_{\rm I}$) 222.65 ($M_{\rm I}$) 222.75 ($N_{\rm I}$)	14.0 ± 1.0 < 3.2 0.63 ~0.16	(5.6)	⩾15	(4)	4 ± 1	
.0 ± 0.2	224.0 (K) 224.1 ($L_{\rm I}$) 224.0 ($M_{\rm I}$) 223.9 ($N_{\rm I}$)	5.2 ± 0.8 0.94 0.24 ~0.08	5.5 ± 0.9	⩾15	4.0 ± 0.8	3 ± 2	
.6 ± 0.2	249.63 (K) 249.58 ($L_{\rm I}$) 249.59 ($M_{\rm I}$) 249.6 ($N_{\rm I}$)	53.0 ± 3.0 9.5 2.4 ~0.6	5.6 ± 0.5	⩾160	3.9 ± 0.4	4.0 ± 0.8	N line interferes with the 338.4 keV K line in Bi^{206}
.0 ± 0.3	288.0 (K) 288.1 ($L_{\rm I}$)	0.9 ± 0.2 0.16	5.6 ± 0.8	—	—	—	
.5 ± 0.2	307.51 (K) 307.45 ($K_{\rm I}$) 307.50 ($M_{\rm I}$) 307.3 ($N_{\rm I}$)	14.0 ± 1.0 2.5 0.59 ~0.2	5.6 ± 0.6	⩾18	4.2 ± 0.6	3 ± 2	N line interferes with 311.5 keV $M_{\rm I}$ line in Bi^{206}
.2 ± 0.3	330.20 (K) 330.28 ($M_{\rm I}$)	4.2 ± 0.5	(4.8)	—	(4)	—	L and N lines hidden by K 405.7 and $L_{\rm I}$ 345.2 lines respectively

Table 1 *(continued)*

Adopted transition energy (keV)	Transition energy calculated from conversion lines (keV)	Relative line intensity (K 405.7 = 100)	$K/\Sigma L$	$(L_{\mathrm{I}}+L_{\mathrm{II}})/L_{\mathrm{III}}$	$\Sigma L/M\Sigma$	$M/(N+O)$	Remarks
345.2 ± 0.2	345.21 (K)	34 ± 3	5.6 ± 0.5	⩾ 90	4.0 ± 0.4	3.4 ± 0.7	
	345.18 (L_{I})	6.0					
	345.19 (L_{III})?	~ 0.06					
	345.18 (M_{I})	1.5					
	345.23 (N_{I})	0.44					
369.3 ± 0.3	369.3 (K)	1.7 ± 0.3	6.0 ± 0.9	—	—	—	
	369.3 (L_{I})	0.29					
402.4 ± 0.4	402.5 (K)	0.90 ± 0.10	5 ± 1	—	—	—	
	402.3 (L_{I})	~ 0.02					
405.7 ± 0.3	405.71 (K)	100	5.7 ± 0.5	⩾ 160	4.1 ± 0.4	3.2 ± 0.6	
	405.74 (L_{I})	18					
	405.62 (M_{I})	4.4					
	405.79 (N_{I})	1.4					
531.7 ± 0.5	531.7 (K)	1.6 ± 0.3	6.4 ± 1.0	—	—	—	
	531.8 (L_{I})	0.25					
629.9 ± 0.4	629.9 (K)	4.5 ± 0.5	6.2 ± 0.6	⩾ 30	3.4 ± 0.6	~ 3	
	629.7 (L_{I})	0.72					
	629.9 (M_{I})	0.22					
	629.5 (N_{I})	0.07					
669.5 ± 0.5	669.5 (K)	1.7 ± 0.2	(6.2)	—	(4)	—	*L* lines coincide w 742.7 keV *K* line
	669.4 (M_{I})	0.07					
687.5 ± 0.7	687.5 (K)	0.48 ± 0.08	6 ± 1	—	—	—	
	687.3 (L_{I})	~ 0.08					
742.7 ± 0.4	742.7 (K)	59 ± 5	6.1 ± 0.6	⩾ 100	4.2 ± 0.4	3.2 ± 0.6	
	742.6 (L_{I})	9.7					
	742.6 (M_{I})	2.3					
	742.8 (N_{I})	0.73					
770.7 ± 0.7	770.7 (K)	0.74 ± 0.10	5.3 ± 0.6	—	—	—	
	770.6 (L_{I})	0.14					
892.4 ± 0.8	892.4 (K)	0.26 ± 0.05	~ 5	—	—	—	
	892.5 (L_{I})	~ 0.05					
911.8 ± 0.5	911.8 (K)	2.6 ± 0.2	5.4 ± 0.8	—	~ 4	—	
	912.0 (L_{I})	0.48					
	912.0 (M_{I})	~ 0.1					
947.8 ± 0.6	947.8 (K)	1.3 ± 0.1	3.2 ± 0.6	—	—	—	*M* line hidden by 103 keV *K* line in Bi
	947.6 (L_{I})	0.41					
992.6 ± 0.5	992.5 (K)	54 ± 4	6.0 ± 0.5	⩾ 80	4.2 ± 0.4	4.0 ± 0.8	
	992.6 (L_{I})	9.2					
	992.8 (M_{I})	2.2					
	992.8 (N_{I})	0.56					
1148.8 ± 0.6	1148.8 (K)	1.50 ± 0.15	5.3 ± 0.5	—	3.6* ± 0.4	—	
	1148.7 (L_{I})	0.28					
	1149.5 (M_{I})	0.078					

le 1 *(continued)*

opted nsition nergy keV)	Transition energy calculated from conversion lines (keV)	Relative line intensity (K 405.7 = 100)	$K/\Sigma L$	$(L_I+L_{II})/L_{III}$	$\Sigma L/\Sigma M$	$M/(N+O)$	Remarks
.6 ± 1.0	1216.6 (K) 1212 (L_I) 1213 (M_I)	0.13 ± 0.02 0.044 ~0.01	3 ± 1	—	4.4* ± 0.5	—	L lines probably superimposed on other lines
.9 ± 2.0	1317.9 (K)	~0.013	—	—	—	—	
.7 ± 1.0	1360.7 (K) 1360.9 (L_I)	0.23 ± 0.03 0.043	5.3 ± 0.5	—	—	—	$M+N$ lines hidden by 1373 keV L lines
.1 ± 1.0	1373.1 (K) 1372.9 (L_I) 1373.4 (M_I)	0.25 ± 0.03 ~0.045 0.018	5.5 ± 0.5	—	2.5* ± 0.6	—	
.1 ± 2.5	1586.1 (K)	0.019 ± 0.004	—	—	—	—	
.7 ± 2.5	1662.7 (K) 1662.2 (L_I)	0.022 ± 0.004 ~0.004	~5	—	—	—	
.7 ± 2.5	1762.7 (K) 1763.7 (L_I)	0.027 ± 0.005 ~0.005	~5	—	—	—	
.0 ± 3.0	1847.0	0.016 ± 0.004	—	—	—	—	
.8 ± 1.2	2060.7 (K) 2061.3 (L_I) 2063.0 (M_I)	0.21 ± 0.03 0.038 0.013	5.5 ± 0.6	—	3.0* ± 0.6	—	

* The N line included in the M line.

these lines may not necessarily belong to the decay of Po^{207}. Some lines, however, correspond to transition energies which would be expected according to the proposed decay scheme. Those lines to which most probable assignments can be given are included in the first part of Table 2.

2.4. *Relative gamma intensities and multipole assignments*

Scintillation spectra were measured with a NaI(Tl) crystal in combination with a single channel pulse-height analyser. In Figures 4 and 5 are shown the low and high energy spectra obtained from a Po^{207} source. The resolution for the 662 keV Cs^{137} gamma ray was 8 %. The photopeaks of the strong transitions, known from the analysis of the conversion lines, are easily identified in the spectra. The places where the photopeaks of some other known transitions should appear are indicated by arrows in the figures. It is apparent from the figures that two or more gamma rays contribute to many of the photopeaks observed. The weak photopeak of about 2600 keV is probably not a sum up peak, as it was observed from a stronger source placed about 50 cm from the crystal.

Though it is difficult to analyse in detail a scintillation spectrum as complex as that from the decay of Po^{207}, rough estimates of the intensities of the stronger

Table 2. Probable assignments of weak conversion lines from the decay of Po^{207}.

Energy of conversion line (keV)	Line intensity (K405.7 = 100)	Probable assignment	Remarks
87.14	2.0	K 177.7	
161.3	0.28	L_{I} 177.7	
123.86	0.75	K 214.4	L_{I} line hiddden by K 288.0
280.6	0.3	L_{I} 297.0	K line hidden by L_{I} 222.7
293.2	0.1	M_{I} 297.2	
299.6	0.65	K 390.1	L_{I} line composite with K 463.5 (Bi^{206})
374.8	~0.2	L_{II} 390.5?	
412.8	0.26	K 503.3	
487.4	0.08	$L_{\mathrm{I}}+L_{\mathrm{II}}$ 503.3	
489.0	0.08	L_{III} 503.3	
607.8	0.20	K 698.3	
1004.0	0.05	L_{I} 1020.4	K line composite with L 947.8
49.20	0.45	K 139.7	
51.49	0.75		
66.39	0.2		
135.9	0.2		
156.1	0.1		
163.0	0.15		
235.9	0.06	L_{III} 249.6?	
238.4	~0.05		
284.0	0.2		
289.6	0.2	K 380.1	
309.5	0.4		
323.4	0.2		
361.8	0.18		
378.0	0.20	K 468.5	
496.8	~0.1		
751.0	~0.05		
864.7	~0.1	K 955.2	
~1190	~0.015	K ~1280	Composite with L 1211.6
1656.3	~0.01	K 1746.8	
1706.2	~0.005	K 1796.7	

gamma rays of importance for the multipole assignments have been made. The intensities in column 2 of Table 3 are derived from the areas of the photopeaks and corrected for the crystal efficiency according to the efficiency measurements of Kahn and Lyon [20]. The Compton background produced by the higher energy gamma rays has been approximated by the use of the scintillation spectra of Y^{88} (1.85 MeV), Na^{22} (1.28 MeV), Cs^{137} (0.662 MeV) and Hg^{203} (0.279 MeV) as distribution shape standards, measured with the same experimental arrangement.

As the multipole order of the gamma ray is intimately connected with the intensities of the conversion electrons in the competing conversion process the multipole assignments will be discussed together with the transition intensities. The multipolarities given in column 4 of Table 3 are based on comparison of measured $K/\Sigma L$ and $(L_{\mathrm{I}}+L_{\mathrm{II}})/L_{\mathrm{III}}$ ratios with the corresponding theoretical ratios, derived by inter-

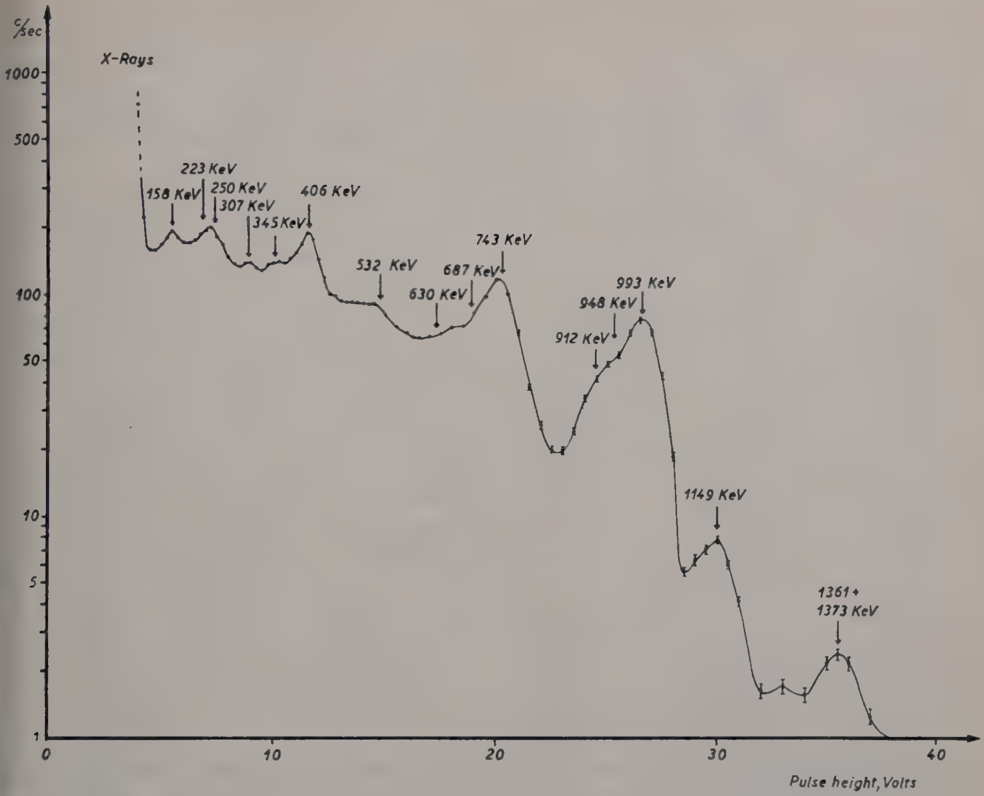

Fig. 4. Scintillation spectrum (low energy part) of Po^{207} gamma rays. Source to crystal distance 3 cm. Channel width 0.5 Volt. Corrected for decay.

polation from the K and L shell conversion coefficients calculated by Rose *et al.* [21], and by comparison of experimental K conversion coefficients with the theoretical coefficients calculated by Sliv *et al.* [22]. Knowing the multipolarity, the relative gamma intensity (I_γ) is determined from the K conversion line intensity (I_K) and the K conversion coefficient (α_K) according to the relation

$$I_\gamma = \frac{I_K}{\alpha_K}.$$

The total transition intensity (I) is given by the gamma intensity and the sum of the intensities of the conversion lines of this transition:

$$I = I_\gamma + I_K + \Sigma I_L + \Sigma I_M + \cdots$$

In order to compare the measured gamma intensities with the gamma intensities derived according to the above formula, both should be expressed in the same units. For this purpose the ratios of the calculated gamma intensities to the measured intensities of the photopeaks at 405, 743 and 990 keV have been derived in Table 4.

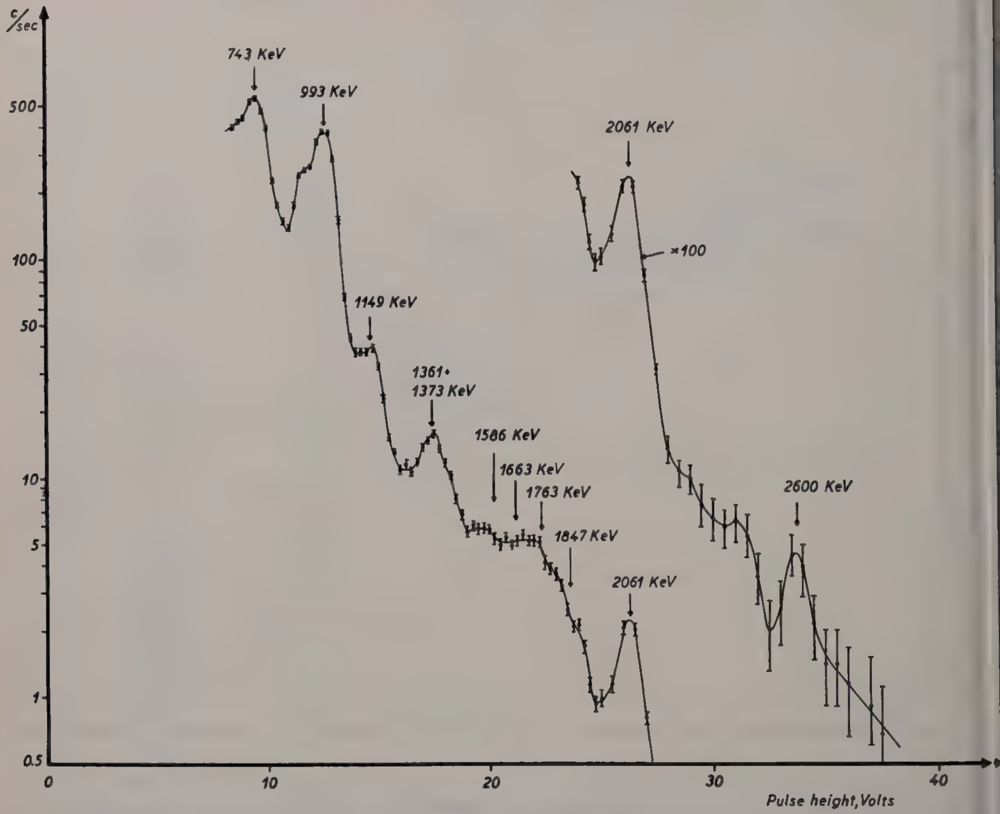

Fig. 5. Scintillation spectrum (high energy part) of Po^{207} gamma rays, measured through a 3.5 g/cm^2 lead absorber. Source to crystal distance 6 cm. Channel width 0.5 Volt. Corrected for decay.

According to the conversion data the 405.7, 742.7 and 992.6 keV transitions are predominantly $M1$ transitions: any other multipolarity is excluded by the large $K/\Sigma L$ and $(L_{\mathrm{I}}+L_{\mathrm{II}})/L_{\mathrm{III}}$ ratios. The 405 and 743 keV photopeaks are predominantly due to the 405.7 and 742.7 keV transitions respectively, since the conversion lines of the interfering transitions are very weak. To the 990 keV photopeak either the 911.8 or the 947.8 keV transition or both should contribute considerably as indicated by the broad photopeak in the scintillation spectra. In the last part of this section it is shown by external conversion measurements, however, that the 911.8 keV transition is of multipolarity $E1$, while the gamma intensity of the 947.8 keV transition is negligible. Using the average ratio from Table 4 the relative gamma intensities tabulated in column 3 of Table 3 were deduced and, as a consequence of the method adopted, are given relative to the K conversion line of the 405.7 keV transition.

The multipolarities of the transitions for which assignments are possible on the basis of the experimental data obtained so far, will now be discussed.

The 100.0 keV transition.—The measured relative L line intensities $L_{\mathrm{I}}:L_{\mathrm{II}}:L_{\mathrm{III}}=$ 7.1:1.2:1.0, compared with the corresponding theoretical ratios 165:14.5:1.0,

Table 3. Intensities and multipolarities of transitions in Bi^{207}.

Gamma energy keV	Measured gamma intensity (K X-rays = 100)	Measured gamma intensity (K 405.7 = 100)	Multipolarity	Calculated gamma intensity (K 405.7 = 100)	Calculated transition intensity (K 405.7 = 100)
100.0			89% $M1$ + 11% $E2$	7.2±0.7	80±8
149.6	1.6±0.5	78±26	$M1$	4.6±0.6	20±3
156.1			$M1$	3.1±0.3	12±1
158.0			8% $M1$ + 92% $E2$	28±3	61±6
205.2			$M1$?	1.1±0.2	2.6±0.3
222.0	5.1±1.5	250±80	$E1$	68±14	73±15
222.7			$M1$	16±1.6	34±3
224.0			$M1$	6.2±0.6	12.5±1.8
249.6			$M1$	84±5	150±9
288.0	1.0±0.5	49±25	$M1$?	2.1±0.3	3.3±0.3
307.5			$M1$	39±3	56±4
330.2	3.6±1.2	176±57	$M1$?	14.5±1.5	20±2
345.2			$M1$	131±12	173±12
369.3			$M1$?	8±1	10±2
402.4	13.0±4.0	640±210	$M1$?	5.3±0.7	6.5±0.7
405.7			$M1$	600	723
531.7			$M1$?	20±3	22±4
629.9			$M1$	85±8	91±10
669.5	36±8	1760±450	$M1$?	40±5	42±5
687.5			$E1$?	108±12	109±13
742.7			$M1$	1730±150	1800±150
770.7			$M1$?	25±3	26±4
892.4			($M1$ + $E2$)?	26±4	26±4
911.8	84±16	4100±900	$E1$	1000±80	1000±80
947.8			$M1$?	73±7	75±7
992.6			$M1$	3400±260	3470±260
1148.8	6.4±1.8	314±95	$E2$	345±35	347±35
1317.9	3.5±1.0	170±53	$M2$?	≈1	≈1
1360.7			$E2$?	75±10	75±10
1373.1			$E2$	80±10	80±10
1762.7			$E2$?	~13	~13
2060.8	1.6±0.4	78±22	$E3$	72±10	72±10
~2600	≈0.05	≈3	—		

Table 4. Ratios of gamma intensities derived from conversion line intensities to measured gamma intensities.

Transition energy keV	Calculated gamma intensity (K 405.7 = 100)	Measured gamma intensity (K X-rays = 100)	Ratio of calculated to measured gamma intensity
405.7 ($M1$)	600	13.0±4	46±14
742.7 ($M1$)	1730±150	36±8	48±12
911.8 ($E1$)	1000±80	84±16	52±10
992.6 ($M1$)	3400±260		
			Mean value 49±6

4.0:0.42:1.0, 2.4:1.0:1.0 and 0.07:1.3:1.0 for $M1$, $M2$, $E1$ and $E2$ respectively, indicate multipolarity $M1$ with some $E2$ admixture. The mixing ratio calculated according to the formula

$$\frac{\gamma_{E2}}{\gamma_{M1}}=\frac{(\alpha_{L_{\mathrm{III}}})_{M1}\left[\left(\frac{L_{\mathrm{I}}+L_{\mathrm{II}}}{L_{\mathrm{III}}}\right)_{\mathrm{exp}}-\left(\frac{L_{\mathrm{I}}+L_{\mathrm{II}}}{L_{\mathrm{III}}}\right)_{M1}\right]}{(\alpha_{L_{\mathrm{III}}})_{E2}\left[\left(\frac{L_{\mathrm{I}}+L_{\mathrm{II}}}{L_{\mathrm{III}}}\right)_{E2}-\left(\frac{L_{\mathrm{I}}+L_{\mathrm{II}}}{L_{\mathrm{III}}}\right)_{\mathrm{exp}}\right]}$$

gives 11 % $E2$.

The 158.0 keV transition.—The measured $K/\Sigma L$ and $(L_{\mathrm{I}}+L_{\mathrm{II}})/L_{\mathrm{III}}$ ratios of 0.75 ± 0.08 and 1.9 ± 0.2 respectively agree best with the theoretical ratios 0.45 and 1.74 for $E2$ transition. Both the experimental ratios are, however, larger than the theoretical ones. An $M1$ admixture of 8.6 % and 6.4 % is obtained from the $K/\Sigma L$ and $(L_{\mathrm{I}}+L_{\mathrm{II}})/L_{\mathrm{III}}$ ratios respectively.

The 149.6, 222.7, 224.0, 249.6, 307.5, 345.2, 405.7, 629.9, 742.7 and 992.6 keV transitions all have measured $K/\Sigma L$ ratios of about 6 and should therefore have the multipolarity $M1$ or $E1$. However, $E1$ is excluded on account of the upper limits of the $(L_{\mathrm{I}}+L_{\mathrm{II}})/L_{\mathrm{III}}$ ratios (cf. Table 1) and their relative gamma intensities. Furthermore, from the $(L_{\mathrm{I}}+L_{\mathrm{II}})/L_{\mathrm{III}}$ limits for the 249.6, 345.2 and 405.7 keV transitions the maximum $E2$ admixture for these transitions is estimated to be less than about 1 %, 5 % and 2 % respectively.

The 156.1 keV transition.—This transition has a $K/\Sigma L$ ratio of about 5.8 and should be assigned as either $M1$ or $E1$, since for any higher multipolarity the $K/\Sigma L$ ratio at this low energy should be less than 3. However, the 1148.8 keV $E2$ transition is most probably the cross-over to the 992.6 and 156.1 keV transitions (cf. section 3.2). The 156.1 keV transition is therefore probably of multipolarity $M1$. The photopeak at 160 keV is a composite of the 149.6, 156.1 and 158.0 keV gamma rays and has the intensity 78 ± 26, while the sum of the 149.6, 156.1 and 158.0 keV gamma intensities is 36 ± 4, if the multipole assignments are correct. The disagreement in intensity may indicate on the presence of other low energy gamma rays. To give an observable contribution to the photopeak, however, the multipolarity of such possible transitions should probably be $E1$, as there are only weak unassigned conversion lines (cf. Table 2).

The 222.0 keV transition.—The L lines of the 222.0 keV transition are superimposed on other lines. However, lines are indicated which could be assigned as L_{I} and L_{III} (cf. section 2.3). The observed K/L_{III} ratio of about 30 indicates an $E1$ or $M2$ transition; higher multipole orders should have smaller K/L_{III} ratios. If the calculated gamma intensities for the 222.7, 224.0 and 249.6 keV transitions are subtracted from the measured intensity of the 250 keV photopeak the resulting gamma intensity 144 ± 80 is obtained. This intensity, if attributed mainly to the 222.0 keV transition, gives the K conversion coefficient $0.025\begin{smallmatrix}+0.030\\-0.010\end{smallmatrix}$. The theoretical values 0.051 and 3.0 for $E1$ and $M2$ transitions respectively suggest multipolarity $E1$ for the 222.0 keV transition.

The 330.2 and 369.3 keV transitions.—The 330.2 keV transition probably has the multipolarity $M1$ (or possibly $M2$). If it were $E1$ its gamma intensity would be about 210 and the gamma intensity of the 330.2 and 345.2 keV transitions together would be more than a half of the 405.7 keV gamma intensity, which is in disagreement with the gamma intensity measurements. For the same reason the 369.3 keV transition is most probably $M1$.

The 911.8 keV transition has multipolarity $E1$ as is shown by the external conversion measurements discussed in the last part of this section.

The 1148.8 keV transition.—The K conversion line intensity compared with the measured gamma intensity gives the experimental conversion coefficient $\alpha_K = 0.0048 \pm 0.0015$ in very good agreement with the theoretical conversion coefficient for $E2$ (theoretical value 0.0044). Moreover, multipolarity $E2$ is supported by the external conversion measurements.

The 1360.7 and 1373.1 keV transitions.—A very weak photoline of energy corresponding to the K line of a 1372 keV transition was found in the external conversion spectrum. If attributed to the 1373 keV transition, the line intensity indicates multipolarity $E1$ or $E2$. As further the 1373.1 keV transition is most probably the cross-over transition to the cascading 629.9 and 742.7 keV $M1$ transitions and to the 1148.8 keV $E2$ and 224.0 keV $M1$ transitions, the multipolarity $E2$ seems plausible. Its gamma intensity should then be 80 ± 10. The measured intensity of the photopeak at about 1370 keV is 170 ± 53 and the gamma intensity of the 1360.7 keV transition should then be 90 ± 54, which gives the K conversion coefficient $\left(2.5 \begin{array}{l} +4.0 \\ -1.0 \end{array}\right) \times 10^{-3}$. The theoretical values for $E1$, $E2$, $E3$ and $M1$ are 1.3×10^{-3}, 3.4×10^{-3}, 6.5×10^{-3} and 7.2×10^{-3} respectively. The experimental conversion coefficient seems thus to indicate multipolarity $E2$ for the 1360.7 keV gamma ray, though $E3$ or $M1$ cannot be quite excluded.

The 2060.8 keV transition.—The measured K line intensity and gamma intensity give the conversion coefficient $\alpha_K = (2.7 \pm 0.9) \times 10^{-3}$. This value agrees best with the theoretical coefficients for either $M1$ ($\alpha_K = 2.6 \times 10^{-3}$) or $E3$ ($\alpha_K = 2.9 \times 10^{-3}$). However, the 2060.8 keV transition is most probably the cross-over transition to the 1148.8 keV $E2$ and 911.8 keV $E1$ transitions. If this is the case, a spin change of either 1, 2 or 3 units with change of parity must be involved and hence the multipolarity should be either $E1$, $M2$ or $E3$. Of these possibilities only the assignment $E3$ agrees with the experimental conversion coefficient.

The measured $K/\Sigma L$ ratios for the 205.2, 288.0, 402,4 and 531.7 keV transitions are compatible with multipolarities $M1$ or $E1$. For these transitions as well as for the remaining weak transitions from Table 1 multipole assignments are impossible on the basis of the present conversion data and relative gamma intensities. For some of them, included in Table 3, probable assignments based on the decay scheme are given (cf. section 3.3).

The broad photopeak observed in the scintillation spectrum at about 990 keV indicates that either the 911.8 or the 947.8 keV transition is only slightly internally converted. A definite multipole assignment is difficult to give on the basis of the data obtained in the investigation of conversion electron and scintillation spectra. Due to the low intensities of the conversion lines and the presence of interfering lines accurate measurements of $K/\Sigma L$ ratios were not possible. However, a determination of the multipolarities of the 911.8 and 947.8 keV transitions, if possible, was considered of importance. Therefore, a measurement of the photoelectrons ejected from an external converter was performed in the double focusing spectrometer.

In Fig. 6 is shown a part of the external conversion spectrum obtained from a strong Po^{207} source using a 10 mg/cm^2 lead converter with the area 3×20 mm^2 and the spectrometer transmission adjusted to about 1 %. The conversion electrons were

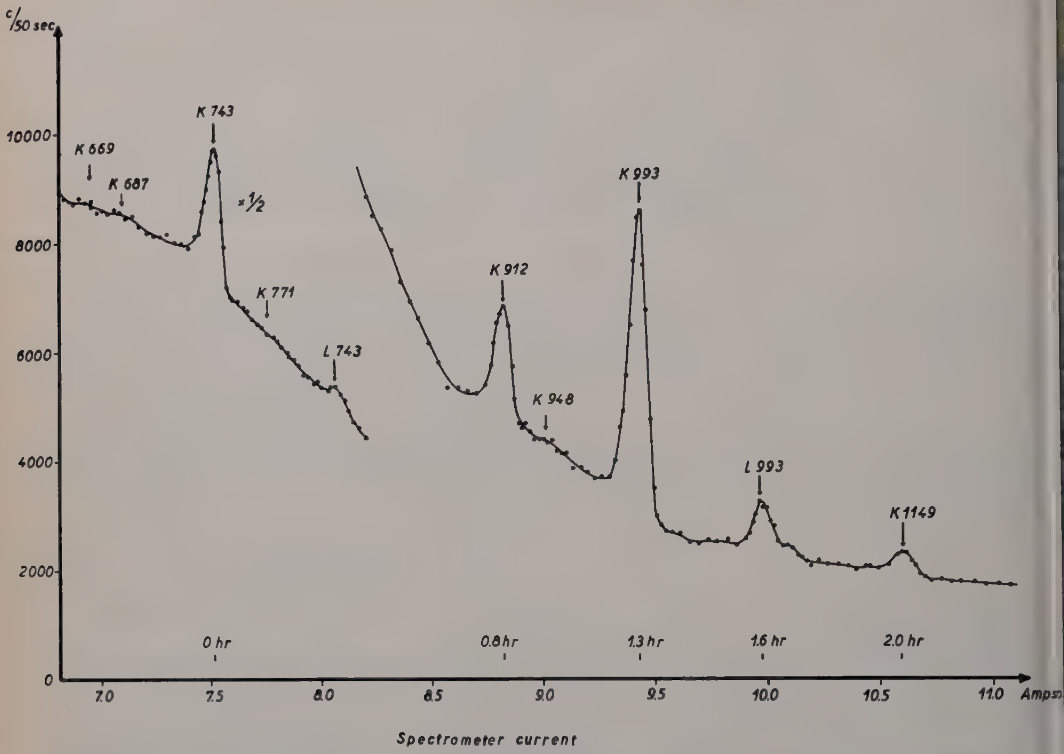

Fig. 6. Photoelectron lines of Po^{207} gamma rays produced in a 10 mg/cm^2 lead converter and measured in the double focusing spectrometer.

stopped by a Cu foil of 1.2 mm thickness. The photolines from the gamma rays of energies 405.7, 742.7, 911.8, 992.6 and 1148.8 keV are easily identified. The places where the K photolines of some other transitions are expected to appear are indicated by arrows in Fig. 6.

The intensity (A_K) of a K photoline is related to the gamma intensity (I_γ) by the relation

$$A_K = k I_\gamma \tau_K,$$

where τ_K is the photoelectric K absorption coefficient for the converter material. The factor k appearing in the formula is in general not a constant on account of the energy dependence of the angular distribution of the ejected photoelectrons. Furthermore, k is dependent on the position of the source relative to the converter, electron scattering and absorption in the converter and the spectrometer transmission. Though difficult to calculate, the variation of k with gamma energy can be experimentally determined for a particular converter arrangement by the use of sources of gamma rays of known multipolarities. In this particular case, however, the multipolarities and relative gamma intensities of the 405.7, 742.7, 992.6 and 1148.8 keV transitions are known from the study of the conversion and scintillation spectra, and the data for these gamma rays can be used for the determination of k.

Table 5. Relative gamma intensity of 911.8 keV transition from external conversion measurements.

Transition energy keV	A_K (arbitrary units)	τ_K (in 10^{-24} cm^2/atom)	I_γ (K 405.7 = 100)	k (arbitrary units)
405.7 ($M1$)	38 ± 5	38.8	600	$(1.63 \pm 0.21) \times 10^{-3}$
742.7 ($M1$)	27 ± 4	9.85	1730 ± 150	$(1.59 \pm 0.28) \times 10^{-3}$
992.6 ($M1$)	30 ± 4	5.37	3400 ± 260	$(1.64 \pm 0.25) \times 10^{-3}$
1148.8 ($E2$)	2.6 ± 0.5	4.10	345 ± 35	$(1.84 \pm 0.38) \times 10^{-3}$
911.8	11.8 ± 2.1	6.36	1100 ± 200	1.68×10^{-3}

The values of k obtained together with the values of A_K, I_γ and τ_K are given in Table 5. In deriving the A_K values the photoline of the 992.6 keV gamma was corrected for the coinciding $L + M$ photoline of the 911.8 keV gamma ray, assuming a $K/(L + M)$ ratio of 5. The τ_K were interpolated from the table of absorption coefficients given by Davisson and Evans [23].

As is seen from Table 5, the values of k are constant within the limits of error. There is, however, a small trend towards larger k values with increasing gamma energy, which would be expected due to the increased probability for ejection of photoelectrons in the forward direction at higher gamma energies [23].

With an average k value of 1.68×10^{-3} the relative gamma intensity 1100 ± 200 is obtained for the 911.8 keV transition. The K conversion coefficient then becomes $(2.36 \pm 0.46) \times 10^{-3}$ in agreement with the theoretical value 2.6×10^{-3} for $E1$ transition.

The K photoline of the 947.8 keV gamma ray is not observed above the Compton background in the external conversion spectrum. Its gamma intensity should therefore be weak compared to the intensities of the 992.6 and 911.8 keV gamma rays. $E1$ and probably even $E2$ radiation for the 947.8 keV transition can therefore be excluded.

2.5. *Positron spectrum*

Stoner [9] observed the emission of positrons in the decay of Po^{207}, but their energy distribution was not measured. As a knowledge of the positron spectrum and feeding is of interest for the construction of the decay scheme, the positron spectrum was studied in the double focusing spectrometer, adjusted for a transmission of about 1.5 %. The spectrum obtained from a strong source is shown in Fig. 7 A. The background (about 4 % of the intensity maximum of the positron distribution) is subtracted in the experimental points. The high energy part of the spectrum was carefully studied in a search for higher energy positron components. As indicated in Fig. 7 A by the ten times magnified high energy part of the spectrum, the intensity of any such component should be low. The decay rate of the positrons was measured in the spectrometer and gave a half-life of about 5.8 hr.

In Fig. 7 B is shown the Fermi plot of the positron distribution. The Fermi functions used in the analysis [24] were corrected for screening. Two partial positron spectra are clearly seen from the shape of the Fermi plot. After subtraction of the high energy component (allowed shape assumed), the resulting experimental points

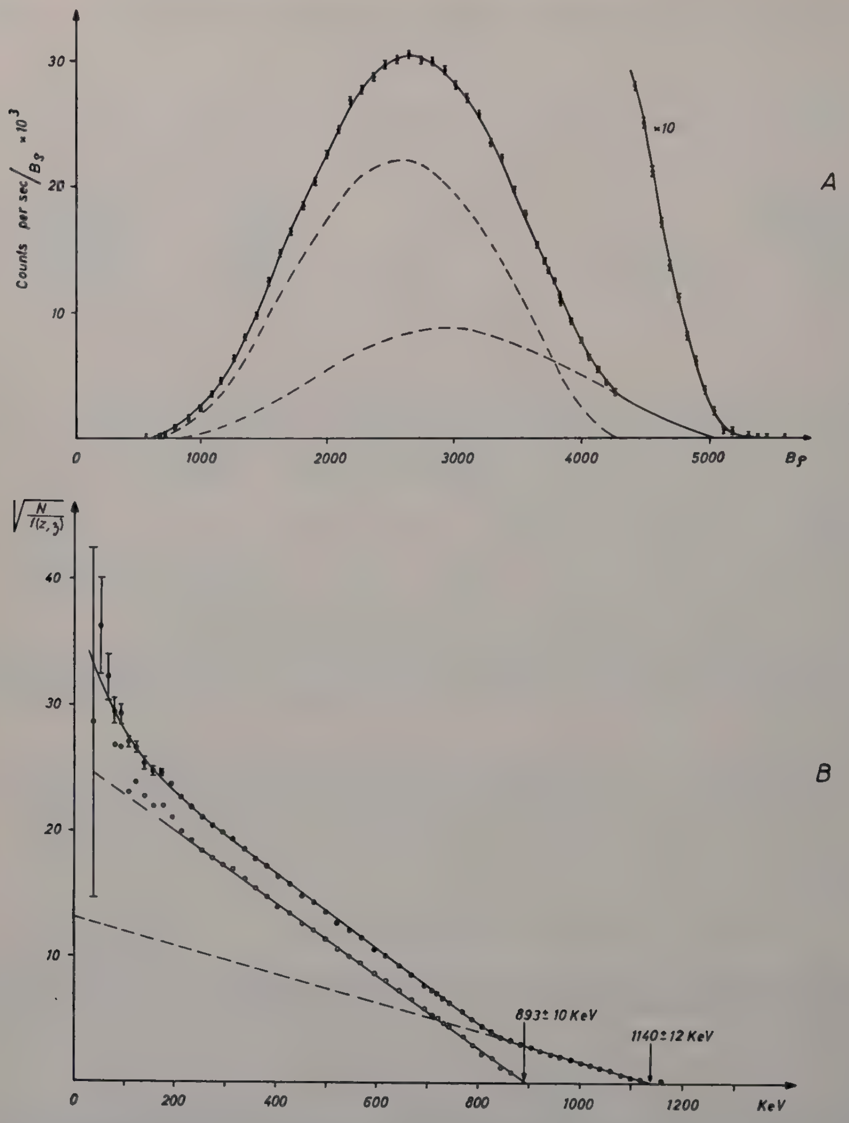

Fig. 7. (A) Positron spectrum of Po^{207} corrected for background and decay. Spectrometer resolution 1.2 %. (B) Fermi analysis of the positron spectrum in (A). The spectrum resolves into two components of end point energies 893 and 1140 keV (dotted in (A)). Allowed shapes are assumed.

lie on a curve which is almost a straight line down to energies less than about 200 keV. Whether the excess of low energy positrons is due to scattering or is an indication of the presence of a low energy positron component is difficult to decide because of the poor statistics.

The positron end point energies for the two components obtained in the analysis

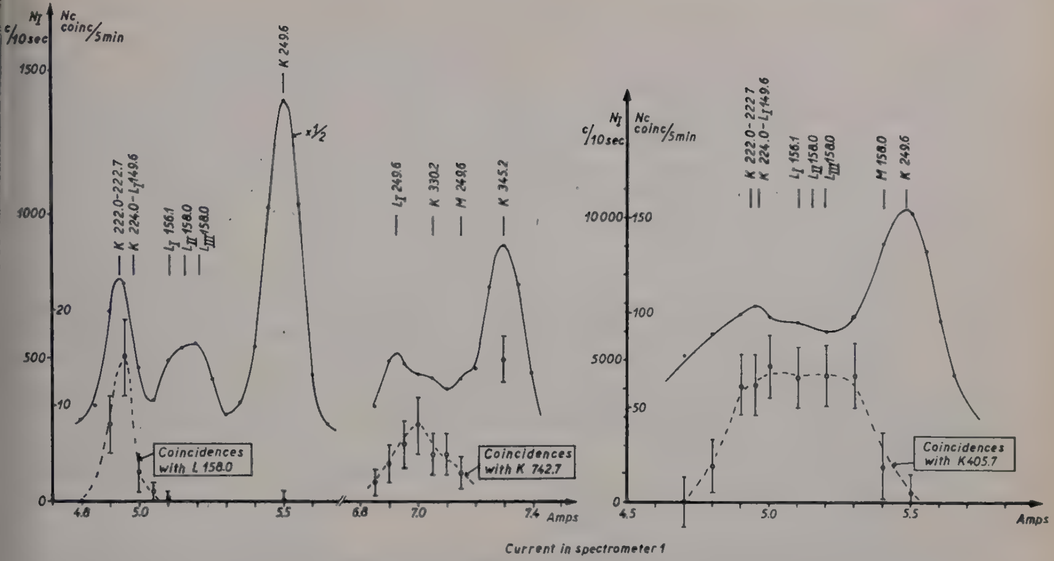

Fig. 8. Coincidences between conversion electrons in the decay of Po^{207} measured in the double lens coincidence spectrometer. The peaks of the conversion lines L 158.0, K 405.7 and K 742.7 are focused in spectrometer 2 when parts of the spectrum are scanned in spectrometer 1. The coincidence lines (dotted curves) are corrected for chance coincidences.

are 893 ± 10 and 1140 ± 12 keV. The total positron intensity, measured relative to the K line of the 1148.8 keV transition, was found to be 29 ± 3 (K $405.7 = 100$). Furthermore, the intensity ratio $\beta^+_{893}/\beta^+_{1140}$ is about 2.1 (both transitions assumed to be allowed). The log ft values are further discussed in section 3.4.

2.6. *Electron-electron coincidence measurements*

In order to construct a plausible decay scheme it is important to know whether definite transitions are emitted in cascade or not. Only limited information would be gained by a study of gamma-gamma coincidences in this case because of the complex gamma-ray spectrum. Moreover, quantitative coincidence data may give the branching ratios and serve to check the validity of the multipolarity for various transitions. Therefore a large number of coincidences between pairs of conversion lines were studied in the double lens coincidence spectrometer [12]. In most measurements the spectrometer was adjusted to 2.5 % transmission in each channel. With a source of 2 mm diameter a resolution of about 2.5 % was then obtained.

In cases where the conversion lines were relatively well resolved the coincidence counting rate was measured when the peaks of the lines were focused in each spectrometer. When the lines could not be resolved, parts of the spectrum in coincidence with a certain line had to be measured. From the shape of the coincidence spectrum thus obtained, it may be judged which lines are most probably in coincidence.

In Fig. 8 is shown the coincidences observed when spectrometer 1 is scanning the energy regions around the K conversion lines to the 222.7 and 330.2 keV transitions, while spectrometer 2 is focused on the peaks of the L lines of the 158.0 and the K lines of the 405.7 and 742.7 keV transitions respectively. It is apparent from Fig. 8 that the L lines of the 158.0 keV transition are in coincidence with the K lines of the 405.7 and the 222.0–224.0 keV transitions but not with the K line of the 249.6 keV transition. The 405.7 keV K line is further seen to be in coincidence with the 222.0–224.0 keV K line group but not with the 249.6 keV K line. The resolution is, however, not good enough to decide about the contribution to the observed coincidence effect from the K conversion lines of the 222.0, 222.7 and 224.0 keV transitions.

The L and M lines of the 249.6 keV transition should be in coincidence with the K line of the 742.7 keV transition as a strong positive coincidence effect was found between the K lines of these transitions. From the shape of the curve in Fig. 8 it is, however, plausible to assume that even the 330.2 keV K line is in coincidence with the 742.7 keV K line. This assumption is further supported by the finding of more coincidences than would be expected due only to the $L+M$ lines of the 249.6 keV transition.

The chance coincidences were measured by introducing in one channel a time delay long compared with the resolving time of the coincidence unit ($2\tau \approx 3\times 10^{-7}$ sec).

The coincidence results obtained from the measurements on 8 sources of various strengths are collected in Table 6. The conversion lines listed first in columns 2 and 3 are assumed to be responsible for the observed effect while lines which could interfere are placed within parentheses. The genuine coincidence counting rate N_c in column 4 is corrected for chance coincidences and the errors given are the standard deviations. Systematic errors or errors due to scattered electrons or gamma rays are not included. Several coincidences were remeasured two or more times, and were generally reproducible.

From the values of N_c one can decide whether two transitions are emitted in cascade or not. By an analysis of the coincidence results, in addition, important information of the branching ratios can be obtained. For this reason the measured coincidences have been analysed according to the simplified formulas

$$N_c \approx N_1 \omega_2 \varkappa_2 \delta_2 \approx N_2 \omega_1 \varkappa_1 \delta_1,$$

where the indices 1 and 2 refer to the conversion line of transition 1, focused in spectrometer 1, and the conversion line of transition 2, focused in spectrometer 2, respectively; N_c is the number of genuine coincidences per unit time; N_1 and N_2 are the peak counting rates of conversion lines focused in spectrometers 1 and 2 respectively; ω_1 and ω_2 are the solid angles in spectrometers 1 and 2; $\varkappa_1$ and $\varkappa_2$ are the conversion probabilities [$\varkappa = \alpha_{\text{line}}/(1+\alpha_{\text{tot}})$] of the conversion lines focused in spectrometers 1 and 2; δ_1 is the part of transition 2 in coincidence with transition 1 and δ_2 is the part of transition 1 in coincidence with transition 2.

In deriving the above formulas, the detector efficiencies are assumed to be constant and equal to unity. Furthermore the effect of angular correlation is neglected.

The solid angle ω_2 was measured by the use of the coincidence data of a Bi^{207} source, and was found to be 2.5 ± 0.3 %. Using this ω_2-value the δ_2-value for the strong coincidence effect between the K lines of the 405.7 and 742.7 keV transitions, measured under identical spectrometer conditions, was found to be 0.87 ± 0.15. It has been assumed therefore that the 405.7 keV transition is in coincidence to

Table 6. Electron-electron coincidences.

Conversion line focused in: Spectrometer 1	Conversion line focused in: Spectrometer 2	N_c coinc/min	δ_2 Measured	δ_2 According to the decay scheme
L158.0 + (M,N156.1)	K222.0(E1) + (K222.7)	3.0 ± 0.8	0.79 ± 0.20	1
L100.0 + (K177.7?)	K222.7(M1) + (K222.0, K224.0, L149.6)	23 ± 1.4	0.28 ± 0.02	0.4
K222.7 + (K222.0)	K224.0(M1) + (L149.6, K222.7, K222.0)	0 ± 0.2	< 0.06	0.01
K687.5 + (K698.3?)		2.4 ± 0.43	0.41 ± 0.10	0.07
L158.0 + (L156.1)	K249.6(M1) + (N158.0, L177.7?)	0.2 ± 0.4	0.01 ± 0.02	0
K307.5 + (M,N222.7)		0 ± 0.4	< 0.03	0
L100.0 + (K177.7?)	K307.5(M1) + (M,N222.7)	− 0.1 ± 0.5	< 0.02	0
L158.0 + (L156.1)		1.2 ± 0.5	0.12 ± 0.05	< 0.7
L100.0 + (K177.7?)	K345.2(M1)	6.4 ± 1.2	0.07 ± 0.02	0
L158.0 + (L156.1)		1.4 ± 0.5	0.03 ± 0.01	0.05
K307.5 + (M,N222.7)		1.6 ± 0.9	0.04 ± 0.02	0.04
K330.2 + (L,M249.6)		0.2 ± 0.2	0.10 ± 0.10	0
L100.0 + (K177.7?)	K405.7(M1) + (K402.4, L330.2)	5.0 ± 1.0	0.20 ± 0.05	0
L158.0		13.4 ± 3.2	0.34 ± 0.11	0.24
K224.0 + (L149.6, K222.7)		12.4 ± 3.2	0.70 ± 0.18	0.67
K249.6 + (N158.0, L177.7?)		4.4 ± 7.4	0.003 ± 0.005	0
K307.5 + (M,N222.7, 224.0)		1.15 ± 0.35	0.13 ± 0.04	0.04
K330.2		0 ± 0.4	< 0.26	0
K345.2		15.3 ± 1.3	0.56 ± 0.06	0.55
K629.9		1.2 ± 0.6	0.12 ± 0.06	0
K911.8		3.8 ± 0.45	0.84 ± 0.12	0.67
L100.0 + K177.7?)	K629.9(M1)	0.6 ± 0.4	0.05 ± 0.04	0
K307.5 + (M,N222.7)		2.9 ± 0.8	0.24 ± 0.06	0.5
K687.5 + (K698.3?)		0.5 ± 0.2	0.55 ± 0.22	0.5
L100.0 + (K177.7?)	K669.5(M1)	2.0 ± 0.4	0.22 ± 0.06	0.4
K222.7 + (K222.0, K224.0)		14.4 ± 1.3	0.95 ± 0.09	1.0
K100.0 + (K177.7?)	K742.7(M1) + (L,M669.5)	3.3 ± 0.9	0.59 ± 0.17	0.25
L158.0 + (L156.1)		3.9 ± 1.4	0.50 ± 0.19	0.6
K205.2		3.1 ± 1.1	1.8 ± 1.0	1.0
K224.0 + L149.6 + (K222.7, K222.0)		11.7 ± 1.7	1.7 ± 0.3	~ 1
K249.6 + (N158.0, L177.7?)		13.5 ± 1.3	0.92 ± 0.09	1.0
K307.5 + (M,N222.7)		0.90 ± 0.25	0.52 ± 0.15	0.5
K330.2 + (L,M249.6)		1.6 ± 0.6	2.9 ± 1.1	1.0
K345.2		4.6 ± 0.6	0.71 ± 0.10	0.6
K405.7 + (K402.4, L330.2)		59.9 ± 2.5	1.00	1.0
K629.9		1.0 ± 0.6	0.69 ± 0.42	1.0
K911.8		1.2 ± 0.3	0.78 ± 0.20	0.67
K992.6 + (L911.8)		1.3 ± 0.6	0.09 ± 0.05	0
L100.0 + (L177.7?)	K911.8(E1)	0.55 ± 0.35	0.37 ± 0.24	0
K345.2		3.14 ± 0.67	0.58 ± 0.15	~ 0.8
L100.0	K992.6(M1) + (L911.8)	− 0.8 ± 1.1	− 0.2 ± 0.3	0
L156.1 + (L158.0)		0.4 ± 1.0	0.8 ± 2.0	0.95
K249.6		− 3.0 ± 1.6	− 0.5 ± 0.2	0
K345.2		0.05 ± 0.3	0.02 ± 0.10	0
K405.7		− 0.4 ± 0.6	− 0.04 ± 0.06	0
K629.9		− 0.4 ± 0.4	− 0.5 ± 0.5	0
K345.2	K1148.8(E2)	1.68 ± 0.44	0.23 ± 0.06	0.25
K687.5 + (K698.3?)	K1373.1(E2) + (K1360.7)	0.05 ± 0.08	0.7 ± 1.0	0.4

100 % with the 742.7 keV transition. This coincidence effect was remeasured and served to evaluate the transmission of the spectrometer for all the sources under investigation, since the transmission of the spectrometer is rather sensitive to the centering and the dimensions of the source.

The $\varkappa$-values necessary for the calculation of the δ's were derived from the conversion coefficients [22], assuming the multipole assignments of Table 3. In the cases where the conversion lines could not be well resolved from interfering lines or the background, the counting rate N_1 (or N_2) has been estimated relative to the counting rate of a stronger resolvable line using the relative line intensities in Table 1.

According to the definition the δ's should be $\leqslant 1$. A small δ-value indicates the occurrence of a considerable branching. The δ_2-values obtained in the analysis of the coincidence data are given in column 5 of Table 6. They will be further discussed in connection with the construction of the decay scheme in section 3.2.

None of the intense transitions in the decay were found in coincidence with the 992.6 keV transition. The gamma-gamma coincidences with the 990 keV photopeak observed by Stoner [9] were probably due to the strong 911.8 keV gamma ray, not observed by him. If this is assumed to be the case, Stoners qualitative coincidence results agree with our measurements.

2.7. *Positron-gamma and positron-conversion electron coincidence measurements*

Both positron-gamma and positron-conversion electron coincidences were studied.

The positron-gamma coincidences were measured in the beta-gamma coincidence spectrometer [13]. The long lens beta spectrometer, provided with helical baffles in order to select between positrons and electrons, was adjusted to the maximum transmission (about 2 %) to detect as much as possible of the weak positron distribution. The positrons were detected by an anthracene crystal. The gamma-ray detector was a 6.25 cm × 5.0 cm NaI(Tl) crystal. The pulses from the gamma-ray detector were fed to the input of the 100-channel analyser and to a coincidence unit with the resolving time $2\tau \approx 3 \times 10^{-8}$ sec. Coincidences between the whole gamma-ray spectrum and the positrons served to gate the multichannel analyser.

In Fig. 9 is shown the number of genuine coincidences accumulated in the multichannel analyser when the beta spectrometer was focusing positrons of energy 428 keV ($B\varrho = 2630$ gauss cm). The curve is obtained by adding the results of 12 consecutive measurements. In each measurement the number of coincidences obtained in 15 min was registered. Thereafter, with an appropiate time delay in the fast coincidence unit, the chance coincidences were measured during 15 min.

In order to calibrate the energy scale of the multichannel analyser without overloading the analyser the field in the beta spectrometer was reversed and the coincidences between the gamma rays and the K conversion line of the 405.7 keV transition were registered in the analyser. From the electron-electron coincidence measurements the 405.7 keV transition was known to be in coincidence with the 742.7 and 911.8 keV gamma rays, and the coincidence peaks of these gamma rays could be used as calibration lines for the analyser.

Though the statistics are poor due to the very low positron intensity, two peaks are indicated in the coincidence curve, corresponding to gamma ray energies of about 745 and 990 keV respectively. Whether the coincidences observed at lower energies are due to the Compton distribution of the 745 and 990 keV gammas or to the photopeak of some lower energy gamma ray is difficult to ascertain. Further-

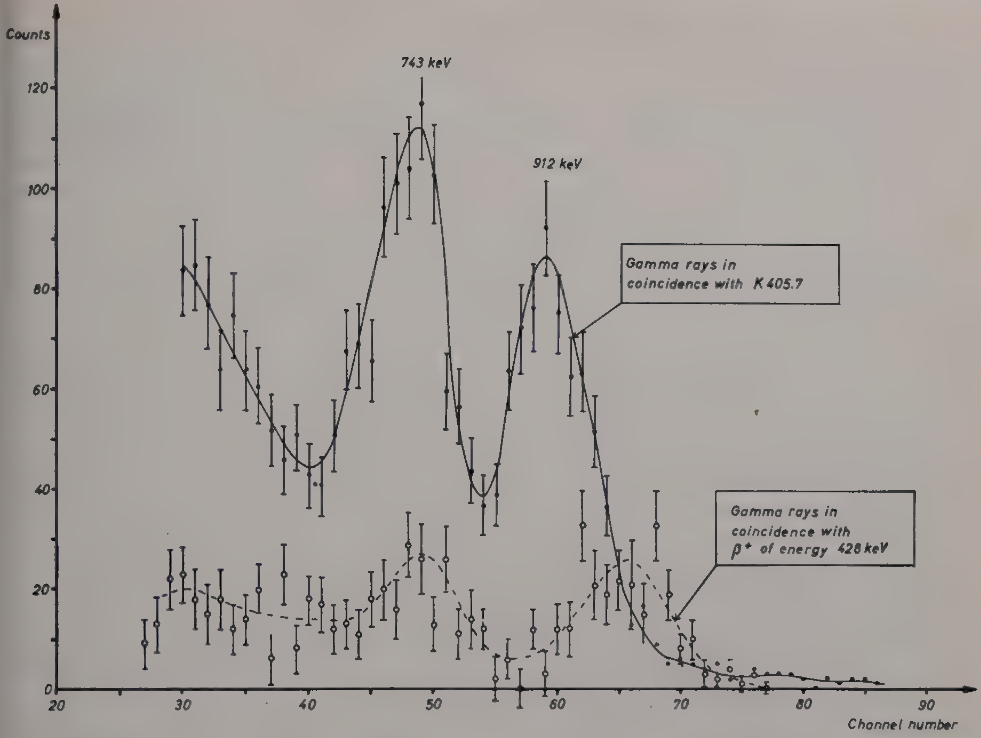

Fig. 9. Positron-gamma and conversion electron-gamma coincidences in Po^{207}. The full curve shows the gamma-ray spectrum in coincidence with the K conversion line of the 405.7 keV transition. The dotted curve shows the coincidences obtained between gamma rays and positrons of energy 428 keV. Chance coincidences are subtracted.

more some of the observed coincidences may be due to the background of scattered gamma rays or electrons in the beta spectrometer.

Coincidences between positrons and K conversion electrons of the strong 405.7, 742.7 and 992.6 keV transitions were studied in the double lens coincidence spectrometer. In order to be able to select either positrons or electrons helical baffles were inserted in the spectrometers. The coincidences were measured when the peaks of the conversion lines were focused in spectrometer 2 and spectrometer 1 was focusing positrons of energies corresponding to the maximum intensity of the positron distribution ($B\varrho = 2600$ gauss cm). The chance coincidences were measured with an appropriate time delay in one channel. The results are summarized in Table 7.

The genuine coincidences N_c in Table 7 are obtained by subtraction of the chance coincidences from the measured total coincidences. The positron counting rates N_1, given for the middles of the long coincidence counting periods, are corrected for the contribution due to gamma background (about 30 %), measured when the positron spectrometer was adjusted for energies above the maximum energy of the positron distribution. With the same spectrometer adjustment coincidences caused by gamma rays were measured. This coincidence effect was found to be small, except for the 405.7 keV line, where the major part of the coincidence counting rate (0.32 ±

Table 7. Coincidences between positrons and conversion electrons.

Conversion line focused in spectrometer 2	N_1 counts/min	N_c counts/min	δ_2 Measured	δ_2 Estimated according to the decay scheme
*K*742.7	1950	0.33 ± 0.21	0.21 ± 0.13	0.27
	1740	0.46 ± 0.19	0.32 ± 0.14	
*K*992.6	1450	0.53 ± 0.16	0.94 ± 0.28	0.73
*K*405.7	1140	0.21 ± 0.24	0.05 ± 0.06	0

0.13 coinc/min) could be ascribed to gamma rays, and was subtracted from the observed coincidence effect for the *K* line of the 405.7 keV transition.

In column 4 of Table 7 the δ_2-values, that is the part of the positrons of momentum 2600 gauss cm in coincidence with the 405.7, 742.7 and 992.6 keV transitions, have been calculated for an estimated transmission of 2.5 %. These δ-values may be compared with the values in column 5, estimated from the positron distribution (cf. Fig. 7) with the assumption that the positrons of maximum energies 1140 and 893 keV feed levels in Bi^{207} de-excited by the 742.7 and 992.6 keV transitions respectively.

The positive coincidence effects observed between positrons and the *K* conversion lines of the 742.7 and 992.6 keV transitions were checked in the same spectrometer, equipped with a fast coincidence unit with resolving time $2\tau \approx 5 \times 10^{-9}$ sec. The *K* conversion lines of the 405.7 and 742.7 keV transitions were focused in spectrometers 1 and 2 respectively and the unit was properly adjusted, using the strong coincidence effect between these lines. Then the current in spectrometer 1 was reversed and coincidences between positrons of energy 406 keV and the *K* conversion line of the 742.7 keV transition were measured. In order to measure coincidences with the 992.6 keV transition the current in spectrometer 2 was increased to focus the 992.6 keV *K* conversion line and the current in spectrometer 1 was appropriately adjusted so that the relative increase in focused energy would be the same in both spectrometers. The results were in fair agreement with the measurements made in the slower coincidence arrangement, thus indicating that the lifetimes of the 742.7 and 992.6 keV transitions are less than about 3×10^{-9} sec.

3. The decay scheme

3.1. *Total decay energy*

The presence of positrons in the decay of Po^{207} and the coincidence measurements enable one to evaluate the total decay energy of Po^{207}. The measurements described in section 2.7 show that the 742.7 and 992.6 keV transitions are both in coincidence with positrons. Then the positions of the levels, fed by positrons, are 743 and 993 keV—or higher—above the ground state of Bi^{207}. However, on account of the following consideration it must be assumed that the levels under discussion have energies of 743 and 993 keV.

According to the coincidence result no. 38 of Table 6, the 742.7 and 992.6 keV transitions cannot be placed in cascade unless one of them has a lifetime long compared to the resolving time of the coincidence unit ($\tau \approx 1.5 \times 10^{-7}$ sec). This is, however, excluded because of the positive coincidence results obtained between positrons and conversion electrons of both transitions with the fast coincidence unit. Since there are no other transitions of comparable intensities observed in the decay, both transitions should lead directly to the ground state from levels of energies 742.7 and 992.6 keV respectively. The energy difference of 250 keV between these levels agrees well with the 253 keV difference between the end point energies of the two positron components observed. Furthermore, a considerable electron capture feeding is expected to the levels fed by the positrons and it will be apparent in the next section that the only levels below about 2 MeV to which an appreciable capture feeding can occur are those of energies about 743 and 993 keV. Finally the measured coincidence effects between the positrons and the 742.7 and 992.6 keV K conversion lines agree quantitatively with what can be estimated from the relative positron intensities (cf. Table 7).

The levels fed by the positrons thus considered to be well established, the total decay energy Q is given by the relation

$$Q = E_L + E_{\beta^+} + 2\,mc^2,$$

where E_L is the energy of the level fed by the positrons, E_{β^+} is the positron end point energy and mc^2 is the electron rest mass energy. The average Q-value, calculated from the two positron branches, is

$$Q = 2.906 \pm 0.008 \text{ MeV}.$$

It should be remarked that Stoner [9] estimated the decay energy as 2.80 ± 0.45 MeV by using the proton and neutron binding energies in a closed energy cycle.

3.2. *Energies of the excited levels*

The 743 and 993 keV levels established in the preceding section by considering the positron feeding constitute a good starting point for the construction of the decay scheme. The observed high energy transitions as well as the 2.9 MeV decay energy indicate that high energy levels occur. In order to find cross-over transitions all possible energy sums of pairs of transitions in Table 1 were calculated and compared with the energy of a third transition. Those cases where the energy sum of two transitions $E_1 + E_2$ is equal to the energy E_3 of another transition within the limits of error, are included in Table 8. Based on energy sum relations, transition intensities, and the analysed coincidence results, the decay scheme shown in Fig. 10 was constructed.

For the following discussion of the levels the reader is referred to Fig. 10 and the Tables 6 and 8. In cases where a certain level is de-excited to the ground state by different branches, the adopted level energy is the weighted average value.

Assuming the existence of levels at 742.9 and 992.5 keV, the 249.6 keV transition should be placed between them in agreement with the sum relation no. 20 (Table 8) and the coincidence results nos. 31 and 43 (Table 6). If there is no branching at the 742.9 keV level, the 249.6 keV transition should be in coincidence to 100 % with the 742.7 keV transition, in good agreement with the measured δ_2-value 0.92 ± 0.09.

Table 8. Transition energy sum relations in Bi^{207}.

Sum No.	E_1 keV	E_2 keV	E_1+E_2 keV	E_3 keV	Stop-over–cross-over relation probable
1	100.0	149.6	249.6	249.6	yes
2	100.0	892.4	992.4	992.6	yes
3	100.0	1662.7	1762.7	1762.7	no
4	149.6	158.0	307.6	307.5	no
5	149.6	742.7	892.3	892.4	yes
6	149.6	1211.6	1361.2	1360.7	no
7	156.1	249.6	405.7	405.7	yes
8	156.1	531.7	687.8	687.5	no
9	156.1	992.6	1148.7	1148.8	yes
10	205.2	742.7	947.9	947.8	yes
11	222.0	770.7	992.7	992.6	no
12	222.0	669.5	891.5	892.4	no
13	222.7	770.7	993.4	992.6	no
14	222.7	669.5	892.2	892.4	yes
15	224.0	307.5	531.5	531.7	yes
16	224.0	405.7	629.7	629.9	yes
17	224.0	687.5	911.5	911.8	yes
18	224.0	1148.8	1372.8	1373.1	yes
19	224.0	1360.7	1584.7	1586.1	no
20	249.6	742.7	992.3	992.6	yes
21	288.0	1373.1	1661.1	1662.7	no
22	345.2	1317.9	1663.1	1662.7	yes
23	369.3	402.4	771.7	770.7	yes
24	369.3	947.8	1317.1	1317.9	no
25	369.3	992.6	1361.9	1360.7	yes
26	402.4	1360.7	1763.1	1762.7	yes
27	405.7	742.7	1148.4	1148.8	yes
28	405.7	911.8	1317.5	1317.9	yes
29	629.9	687.5	1317.4	1317.9	yes
30	629.9	742.7	1372.6	1373.1	yes
31	669.5	992.6	1662.1	1662.7	no
32	687.5	1373.1	2060.6	2060.8	yes
33	770.7	892.4	1663.1	1662.7	no
34	770.7	992.6	1763.3	1762.7	yes
35	742.7	1317.9	2060.6	2060.8	yes
36	911.8	1148.8	2060.6	2060.8	yes

The level at 1148.6 keV is proposed according to the energy sums nos. 7, 9 and 27 and agrees with the measured coincidences nos. 16, 35 and 45.

The 2060.4 keV level is determined by the coincidence effects nos. 21, 35 and 37 and the energy sums nos. 35 and 36. The observed coincidences nos. 21, 35 and 37 could be explained as well if the 405.7 keV transition were feeding the 742.9 keV level indirectly via the strong 911.8 keV *E*1 transition. Then, however, the energy sums nos. 27 and 36 would be accidental. It would furthermore be difficult to explain the observed coincidences between the 345.2 and 1148.8 keV transitions (no. 47) and other coincidences observed with the 405.7 and 742.7 keV transitions. Therefore the succession proposed in Fig. 10 is the most plausible one. According to the level scheme the 911.8 keV transition should be in coincidence with the 1148.8 keV

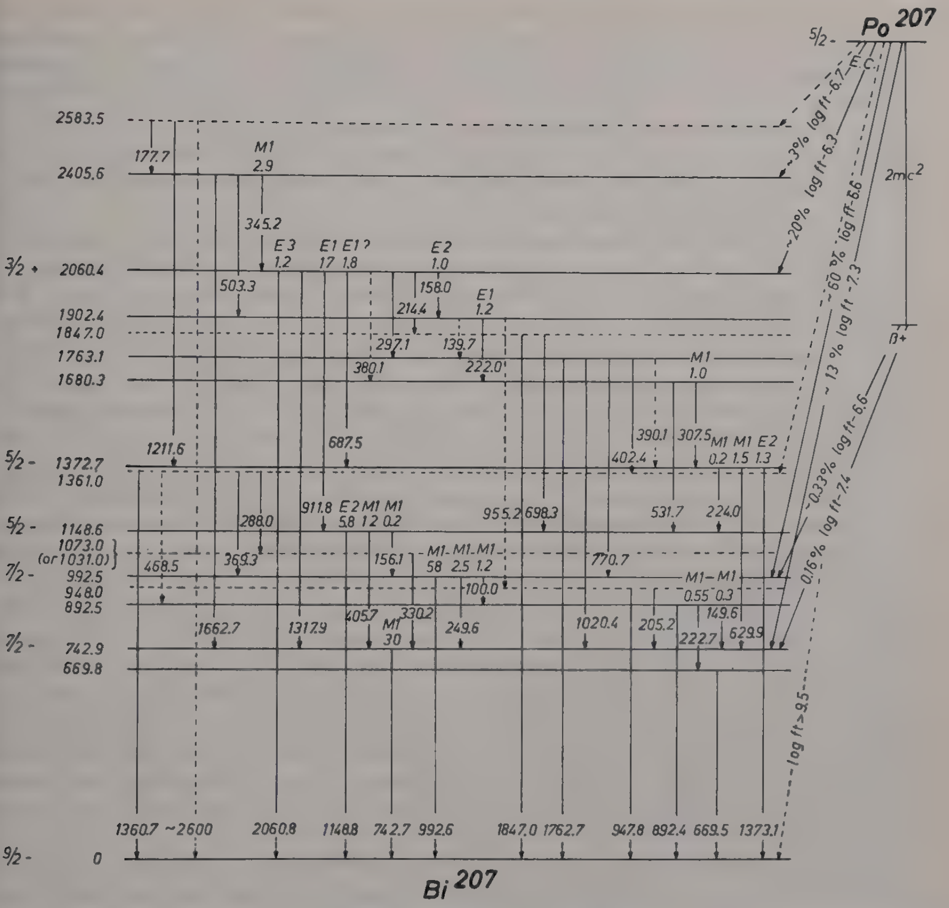

Fig. 10. Proposed decay scheme of Po^{207}. Multipolarities and intensities in per cent per disintegration are given at the head of some transitions. Less certain levels and transitions are indicated by dotted lines. The 992.5 and 742.9 keV levels are fed by positrons of end point energies 893 and 1140 keV respectively.

transition to about 30 %. On account of the low intensities of the K conversion lines, however, this coincidence was not measured.

The positive coincidences nos. 19, 34 and 40 show that the 345.2 keV transition strongly feeds the 2060.4 keV level. For intensity reasons the 345.2 keV transition is assumed to lead directly to the 2060.4 keV level, giving the level at 2405.6 keV. The weak 1662.7 keV transition can then be placed between the 2405.6 and 742.9 keV levels in accordance with the sum relation no. 22.

The levels at 742.9, 992.5, 1148.6, 2060.4 and 2405.6 keV discussed above involve in their de-excitation all the transitions of appreciable intensities observed in the decay of Po^{207} (cf. Table 3). These levels are considered to be very well established. A number of other levels are, however, predicted by the numerous transitions observed and not placed in the level scheme so far.

The level at 1372.7 keV is proposed according to the energy sums nos. 16, 18 and 30 and the positive coincidence effects nos. 15, 30 and 36. The weak coincidences observed between the 629.9 and 405.7 keV transitions (no. 20) cannot be explained by the assumed position of the 629.9 keV transition and indicate that this transition should originate from a higher energy level. However, with the position assumed all the energy sums containing the 629.9 keV transition are accounted for, and the coincidences between the 742.7 keV transition and transitions feeding the 1372.7 keV level can be rather well explained.

The 158.0 and 307.5 keV transitions should, according to the measured coincidences nos. 5, 6, 10, 11, 14, 17, 28 and 32, be placed either above the 2405.6 keV level or between the 2060.4 and 1148.6 keV levels. If placed above the 2405.6 keV level they should feed this level very weakly as is born out by the small δ_2-values obtained from the analysis of the coincidences nos. 10 and 11. Therefore the 158.0 and 307.5 keV transitions are assumed to be fed from the 2060.4 keV level in which case the coincidences with the 345.2 keV transition should be weak, due to the strong 911.8 keV transition. Furthermore the 158.0 and 307.5 keV transitions seem to be in coincidence (no. 8). These considerations together with the positive coincidence no. 1 and the energy sum no. 15 lead to the assumption that the 158.0, 222.0 and 307.5 keV transitions are in cascade between the 2060.4 and 1372.7 keV levels, giving the levels at 1680.3 keV and 1902.4 keV. The probable 503.3 keV transition (cf. Table 2), which may be the cross-over to the 158.0 and 345.2 keV transitions, suggests that the 158.0 keV transition should precede the 222.0 keV transition. The small δ_2-values obtained for the coincidence effect between the 158.0 and 307.5 keV transitions, indicates a considerable branching at either the 1902.4 or the 1680.3 keV levels. Branching at the 1680.3 keV level is compatible with the energy sums nos. 8 and 15. However, the 687.5 keV transition could instead be placed between the 2060.4 and 1372.7 keV levels in accordance with the sum relations nos. 17, 29 and 32, and this is assumed in the proposed level scheme. Its position cannot be decided upon from the coincidence measurements made, although the latter position is supported by the coincidence no. 24.

The only transition not placed so far for which there is a considerable amount of coincidence data available is the 100.0 keV transition. Weak positive coincidence effects were observed with the 345.2, 405.7 and 911.8 keV transitions (nos. 9, 13 and 39) and somewhat stronger effects with the 222.7, 669.5 and 742.7 keV transitions (nos. 2, 25 and 27). This might indicate that the 100.0 keV transition should feed a high energy level. However, the L conversion lines of the 100.0 keV transition are not resolved from the KMM Auger lines and a conversion line which is probably the K line of a 177.7 keV transition (cf. Table 2), and these lines may contribute to the observed coincidence effects. Therefore the 100.0 keV transition is assumed to feed a level at 892.5 keV from the 992.5 keV level, in agreement with the energy sums nos. 1, 2 and 5 and supported by the observed positive coincidences nos. 2, 25, 26 and 27.

The level at 669.8 keV is then proposed according to the sum relation no. 14 and the observed coincidences nos. 2, 3, 25 and 26. If the succession of the cascading 222.7 and 669.5 keV transitions is reversed one would obtain the level energy 222.7 keV instead of 669.8 keV, and the 222.7 keV level could be fed from the 992.5 keV level by the 770.7 keV transition according to the energy sum no. 13. For intensity reasons, however, this seems less probable, since the 222.7 keV transition according to the conversion data should be of predominantly $M1$ character. Thus the energy sum relation no. 13 is probably accidental.

The proposed levels at 1073.0 (or 1031.0) and 948.0 are partly supported by the coincidence results nos. 29 and 33. For the levels at 1361.0, 1763.1 and 1847.0 keV there is no coincidence information available due to the very weak transitions involved in the feeding and de-exciting of these levels. The 1763.1 and 1847.0 keV levels could be fed from the 2060.4 keV level by the probable 297 and 214 keV transitions (cf. Table 2). Furthermore, there are very probably present transitions of energy about 1020 and 698 keV (cf. Table 2), which fit between the 1763.1 and 742.9 keV levels and the 1847.0 and 1148.6 keV levels respectively.

Finally one might assume a level at 2583.5 keV in accordance with the weak gamma ray of about 2600 keV indicated in the scintillation spectrum. This level could then partly be de-excited by the 177.7 and 1211.6 keV transitions to the 2405.6 and 1372.7 keV levels respectively.

The only transition of Table 1 which has not been included in the proposed level scheme is the weak 1586.1 keV transition. This transition occurs only in one energy sum relation (no. 19), which, however, seems to be accidental. The most probably present transitions in Table 2 can also be placed. The energies for a certain level, obtained by considering the different de-exciting possibilities to the ground state, agree very satisfactorily; generally the differences in energy are a few parts in 10000. 11 of the proposed 16 levels are considered as well established, while the remaining 5 levels are less certain since they could not be checked by coincidence measurements for intensity reasons. These levels, and probable transitions from Table 2 whose energies agree with the level spacings, are shown in Fig. 10 by dotted lines.

The branching ratios estimated on the basis of the proposed level scheme and the transition intensities of Table 3 are included in column 6 of Table 6. The agreement between the estimated δ_2-values and those calculated from the coincidence measurements is satisfactory in most cases. In some cases, however, especially where weak transitions are involved, the agreement is not so good but is considered reasonable since the intensities of many weak transitions are uncertain and weak unobserved feeding and de-exciting branches are possible. Furthermore, the calculated δ_2-values may be too large, due to the contribution in the observed coincidence counting rate of unresolved lines.

3.3. *Spin and parity assignments*

The ground state spin of Bi^{207} has not been measured. However, most probable assumption of the spin can be made on the basis of the shell model and on analogy with other odd Bi-isotopes. Bi^{207} has one proton outside the closed shell of 82 protons and two holes in the 126 neutron shell. The ground state spin should then be determined by the odd proton, which is assumed to occupy an $h_{9/2}$ state. The spin 9/2 has been measured for the stable Bi^{209} nucleus [25] and recently also for the Bi^{203} and Bi^{205} nuclei [26]. The $h_{9/2}$ assignment for the ground state of Bi^{207} is further compatible with the electron capture decay of Bi^{207} [27] and seems therefore very probable.

The fact that positrons are feeding excited levels of Bi^{207} but no positrons of observable intensities have been found to the ground state, suggests that the spin difference between the ground states of Bi^{207} and Po^{207} is at least two units. The ground state spin of Po^{207} is therefore probably $\leqslant 5/2$, since the highest odd neutron states do not tend to occur as ground state levels [28].

The 742.9 and 992.5 keV levels.—Both these levels are fed by positrons and should

Table 9. Level feeding and de-excitation in Bi^{207}.

Level energy keV	Intensity of ($K405.7 = 100$):				Electron capture in % per disintegration	log ft
	de-exciting transitions	feeding from higher energy levels	positrons	electron capture		
2405.6	185	—	—	~185	~3	~6.7
2060.4	1350	175	—	1180	20	6.3
1902.4	~73	~74	—	—	—	—
1680.3	78	73	—	—	—	—
1372.7	180	170	—	—	—	—
1148.6	1080	1040	—	—	—	—
992.5	3700	~50	19.6	3630	61	6.6
892.5	~80	~80	—	—	—	—
742.9	1800	1000	9.4	790	13	7.3
0	—	5990	⩽0.4	⩽5	⩽0.1	⩾9.5

therefore have lower spins than the Bi^{207} ground state. As the levels are de-excited to the ground state by the 742.7 and 992.6 keV transitions of predominantly $M1$ multipolarities, the spins of both levels are most probably $7/2-$.

The 1148.6 keV level.—This level is mainly de-excited to the ground state by the cascading 405.7 and 742.7 keV $M1$ transitions and the 1148.8 keV transition, which seems to have multipolarity $E2$. Possible spins are $5/2-$, $7/2-$ and $9/2-$. The strong feeding from the 2060.4 keV level suggests the spin assignment $5/2-$.

The 2060.4 keV level.—The spin $3/2+$ for this level is compatible with the observed 2060.8 keV $E3$ transition to the ground state and the 911.8 keV $E1$ transition to the 1148.6 keV $5/2-$ level. The weak 1317.9 keV transition which probably feeds the 742.9 keV level from the 2060.4 keV level could then have multipolarity $M2$. The experimental ratio of the 911.8 keV gamma intensity to the gamma intensity of the 2060.8 keV transition is 14:1, while a ratio of about $2 \times 10^7:1$ is expected according to the theoretical gamma transition probabilities [29]. The 911.8 keV $E1$ transition probability should then, if the level and multipole interpretation is correct, be considerably slower than theoretically predicted. However, numerous retarded $E1$ transitions have been found [30].

The 892.5 keV level.—Possible spins are $5/2-$, $7/2-$ or $9/2-$, because the 100.0 and 149.6 keV transitions from the 992.5 and to the 742.9 keV levels respectively are of predominantly $M1$ character. As the level is only weakly excited, the most plausible spin seems to be $9/2-$. The 892.4 keV transition could then be of multipolarity $M1$ with a possible $E2$ admixture.

The 669.8 keV level.—Assuming the spin $9/2-$ for the 892.5 keV level the spins $7/2-$, $9/2-$ or $11/2-$ are possible for the proposed 669.8 keV level, because the 222.7 keV transition is $M1$. For the same reason as for the 892.5 keV level, however, the assignment $9/2-$ or $11/2-$ should probably be preferred. The 669.5 keV transition to the ground state could then be an $M1$ transition.

The 1372.7 keV level.—The spins $5/2-$ or $7/2-$ are possible because the level is de-excited by the 224.0 and 629.9 keV $M1$ transitions to the 1148.6 and 742.9 keV levels respectively. The spin $5/2-$ is assumed due to the feeding from the 1680.3

keV level and the indicated $E2$ character of the 1373.1 keV transition to the ground state. Then the 687.5 keV transition should have multipolarity $E1$. However, its position in the level scheme is not quite certain (cf. section 3.2.).

The 1680.3 keV level.—This level is de-excited to the 1148.6 and 1372.7 keV levels by the 531.7 and 307.5 keV transitions respectively which both seem to be $M1$ transitions and can then have the spin $3/2-$, $5/2-$ or $7/2-$. The spin $3/2-$ should probably be preferred because no transition to the 742.9 keV $7/2-$ level has been observed.

The 2405.6 and 1902.4 keV levels.—Both these levels should have positive parity with possible spin values 1/2, 3/2 or 5/2, due to the 345.2 keV $M1$ and the 158.0 keV mixed $M1+E2$ transitions to and from the 2060.4 keV $3/2+$ level respectively. No definite assignment is possible although the spins $3/2+$ or $5/2+$ for the 2405.6 keV level seem preferable because of electron capture feeding from the ground state of Po^{207}.

In the de-excitation of the levels of energies 948.0, 1073.0, 1361.0, 1763.1, 1847.0 and 2583.5 keV only weak transitions are involved. The assignment of spins to these levels is impossible because of the lack of multipolarity data.

3.4. *Electron capture feeding and log ft values*

From the decay scheme of Fig. 10 and the transition intensities of Table 3 the feeding by electron capture of levels in Bi^{207} can be estimated. The difference in intensity between the de-exciting and feeding transitions of a certain level should be balanced by electron capture or by positron emission from the ground state of Po^{207}. The feeding of the most strongly populated excited levels is given in Table 9. Though the level feeding is doubtful to some extent due to uncertainties in the transition intensities, it is apparent from Table 9 that the electron capture leads mainly to the 742.9, 992.5, 2060.4 and 2405.6 keV levels.

The upper limits for positron emission and electron capture to the ground state were estimated in the following way. From the measurement of the positron spectrum it could be concluded that a positron component of end point energy about 1880 keV and with an intensity of 1/80 of the total positron intensity would have been observed above the background. The possible intensity of positrons to the ground state should thus be $\leqslant 0.4$ (K 405.7 = 100). Using the K capture to positron ratio for allowed transitions, as calculated by Zweifel [31], the intensity of electron capture was estimated to be $\leqslant 5$.

The log ft values for the positron and capture decays have been estimated with the aid of Moszkowski's nomogram [32], assuming a total decay energy of 2.91 MeV. The values deduced for capture feeding to various levels are included in Table 9. Assuming a total decay intensity of 6000 (K 405.7 = 100), the intensities of the positrons to the 742.9 and 992.5 keV levels become 0.16 % and 0.33 % per disintegration, corresponding to partial half-lives of about 150 and 70 days respectively. The log ft values 7.4 and 6.6 obtained for the positron transitions to the 742.9 and 992.5 keV levels are in good agreement with the values deduced for electron capture to these levels.

From the intensities of positron and electron capture feeding of the 992.5 and 742.9 keV levels, given in Table 9, the experimental capture to positron ratios become 185 and 83 respectively. These values are in fair agreement with the theoretical ratios 155 and 65 for allowed transitions, obtained by interpolation in Zweifel's table of

K capture to positron ratio [31], and corrected for L capture (L_I to K capture $= 0.15$ assumed) according to the curves given by Brysk and Rose [33].

Transitions with log ft values about 6 or 7 are normally classified as first forbidden or allowed l-forbidden transitions [28], while second forbidden transitions have larger log ft values. It seems reasonable to assume that the decays to the 742.9 and 992.5 keV 7/2 − levels are of the allowed or first forbidden type with spin changes $\leqslant 1$. This assumption is compatible with the shape of the positron distributions (cf. section 2.5) and the capture to positron ratios. First forbidden transitions with spin changes of two units are certainly quite excluded, because then capture to positron ratios of about 700 and 260 for the transitions to the 992.5 and 742.9 keV levels respectively would be expected according to recent calculations by Zweifel [34]. Moreover, the lower limit of the derived log ft value for decay to the ground state indicates a spin change $\geqslant 2$ between the ground states of Po^{207} and Bi^{207}. Therefore, assuming the assignment 9/2 − for the ground state of Bi^{207}, the ground state spin of Po^{207} is very probably 5/2. Odd parity is predicted by the shell model.

4. Discussion

The investigation of the levels in Bi^{207} from the decay of Po^{207}, discussed in the previous sections, has resulted in the construction of a decay scheme containing 16 levels. The main decay of Po^{207} proceeds via the four strongly excited levels of energies 2060.4, 1148.6, 992.5 and 742.9 keV. The observation of transitions from these levels directly to the ground state enabled fairly certain spin assignments to be made. Other levels are only weakly excited. The two levels at 992.5 and 742.9 keV have been found to be strongly fed by electron capture and to some extent by positrons from the ground state of Po^{207}.

As the Bi^{207} nucleus differs from the double magic Pb^{208} nucleus by only three nucleons, one would expect that the levels in Bi^{207} and the main features of the decay would be predicted by the single-particle shell model. It is obvious, however, that the observed levels cannot be ascribed only to pure single-particle states. Complex levels due to coupling in different ways of the extra proton to the neutron holes are possible. It is therefore interesting to compare our experimental levels with those calculated assuming each extra nucleon to occupy a single-particle state. Fig. 11 shows energies and spins of low energy levels for some possible configurations in Bi^{207} as calculated by Wahlborn [7, 35], following the principles introduced by Pryce [2, 3, 4]. The parameters used in the calculation were obtained from Pryce's works on Pb^{206} and Pb^{205}. Configuration mixing was not taken into account. The lowest predicted level has the spin 9/2 − (ground state) and above about 0.6 MeV a large number of levels of various spins are predicted. Two general features of the calculation in agreement with the experiment will be pointed out: (1) All levels below about 1.7 MeV should have odd parities. (2) No level of spin $< 5/2$ is predicted below about 1.5 MeV.

Configuration assignments to the observed levels are difficult to give due to the fact that there are more low-lying levels predicted by the calculations than have been experimentally found. As levels of equal spins from different configurations are predicted to lie close together (cf. Fig. 11) configuration mixing is probably very important. Recent calculations of the energy levels in Pb^{206} by Kearsley [5] and by True and Ford [6], using harmonic oscillator wave functions, show that configuration mixing and level shifts due to configuration interaction may be quite

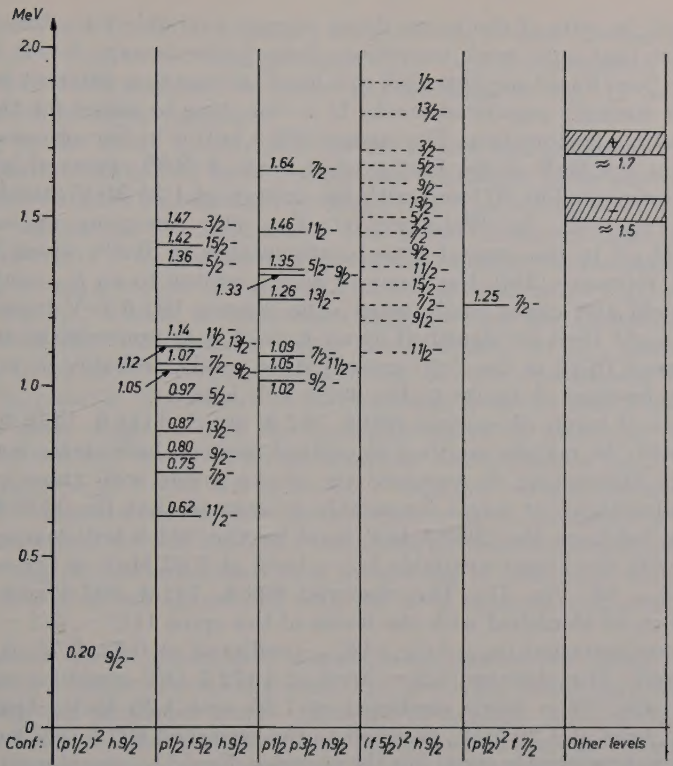

Fig. 11. First order energy levels of Bi^{207} as given by Wahlborn. The calculation was performed with δ-forces and with the aid of Pryce's interaction parameters. The dotted levels in the fourth column are only roughly estimated. In the last column the estimated lower limits for the distribution of all other levels of positive and negative parities have been indicated. The configuration mixing has not been taken into account.

considerable. The following discussion of the probable configuration of various levels, suggested in order to attempt to interpret the observed decay mode of Po^{207}, should therefore be considered as highly tentative.

Po^{207} has two protons outside the closed shell of 82 protons and three holes in the 126 neutron shell. The extra protons are assumed to occupy the $h_{9/2}$ state, coupling their angular momenta to zero resultant. The neutron hole configuration $(p_{1/2})^{-2}$ $(f_{5/2})^{-1}$, with one and two neutrons missing in the $f_{5/2}$ and $p_{1/2}$ orbitals respectively, is compatible with the experimentally indicated spin of 5/2 (cf. section 3.4) and the proposed configurations for the ground states of the nuclei Pb^{205} [4] and Bi^{206} [7], which have the same number of holes in the 126 neutron shell. The electron capture and positron decay of Po^{207} whould then result in the conversion of one of the $h_{9/2}$ protons into an $f_{5/2}$ neutron, assuming $(p_{1/2})^{-2}h_{9/2}$ as the ground state configuration of Bi^{207}. The direct transition $h_{9/2} \rightarrow f_{5/2}$ to the ground state of Bi^{207} would be second forbidden ($\Delta I = \Delta l = 2$, no) and would probably not occur to an observable extent (cf. section 3.4).

The 992.5 keV 7/2 − level is fed about 5 times more from Po^{207} than the 742.9

keV 7/2 − level, in spite of the larger decay energy available for a transition to the latter. The fact that only weak transitions from higher energy levels to the 992.5 keV level have been found suggests that this level belongs to a different configuration from the other strongly populated levels. It is tempting to assign for this level predominantly the $f_{7/2}$ proton state. The energy 992.5 keV is in fair agreement with the energy of about 0.9 MeV of the first excited level of Bi^{209} observed in $Bi^{209}(n;n\gamma)$ scattering experiments [36, 37] and with the energy of 1.25 MeV calculated for the configuration $(p_{1/2})^{-2}f_{7/2}$ by Wahlborn (cf. Fig. 11). Assuming an admixture of $(p_{1/2})^{-2}(f_{5/2})^{-1}(f_{7/2})^{2}$ in the ground state configuration of Po^{207}, which seems quite reasonable (cf. reference [38]), the decay of an $f_{7/2}$ proton to an $f_{5/2}$ neutron of Bi^{207} would be allowed and might easily occur. The intense 992.6 keV transition to the ground state could then be identified as an $f_{7/2} \rightarrow h_{9/2}$ proton transition. A few per cent admixture of $(f_{7/2})^{2}$ in the Po^{207} ground state would probably be enough to explain the large fraction of decays to the 992.5 keV level.

The sequence of levels of energies 669.8, 742.9, 892.5, 1148.6, 1372.7, and 1680.3 keV can probably be mainly ascribed to excited neutron hole states coupled to the $h_{9/2}$ proton. In attempting to correlate the above levels with those predicted by Wahlborn's calculations it seems reasonable to assume that the 1148.6 keV 5/2 − level, strongly fed from the 2060.4 keV level by the 911.8 keV transition, should be identified with the lowest available 5/2 − level at 0.97 MeV of the configuration $(p_{1/2})^{-1}(f_{5/2})^{-1}h_{9/2}$ (cf. Fig. 11). The observed 699.8, 742.9, 892.5 and 1680.3 keV levels could then be identified with the levels of the spins 11/2 −, 7/2 −, 9/2 −, and 3/2 − of the configuration $(p_{1/2})^{-1}(f_{5/2})^{-1}h_{9/2}$, predicted at 0.62, 0.75, 0.80 and 1.47 MeV respectively. The observed 5/2 − level at 1372.7 keV could be one of—or an admixture of—the 5/2 − levels predicted at 1.35 and 1.36 MeV. Apart from the $[(p_{1/2})^{-2}f_{7/2}]_{7/2-}$ level at 1.25 MeV, ascribed to the observed 992.5 keV level, the level order would thus be correctly given but the energies should be considerably perturbed.

With the level assignments suggested, the observed cascading transitions from the 1680.3 keV level and downwards can be rather well explained. However, the 156.1 keV $M1$ transition between the 1148.6 and 992.5 keV levels and the transitions from the latter level to the 892.5 and 742.9 keV levels indicate that the configurations for the 742.9 and 992.5 keV levels are mixed. The presence of an admixture of $[(p_{1/2})^{-2}f_{7/2}]_{7/2-}$ in the configuration of the 742.9 keV level could then be responsible for the observed feeding of this level from the Po^{207} ground state. Moreover, the observed transition of predominantly $M1$ character from the 742.9 keV level could then proceed because of the $[(p_{1/2})^{-2}f_{7/2}]_{7/2-}$ admixture in this level or due to admixtures of $[(p_{1/2})^{-1}(f_{5/2})^{-1}h_{9/2}]_{9/2-}$ or $[(p_{1/2})^{1-}(p_{3/2})^{-1}h_{9/2}]_{9/2-}$ in the ground state configuration of Bi^{207}.

The strongly fed 3/2 + level at 2060.4 keV is preferentially de-excited to the 1148.6 keV 5/2 − level, the 1317.9 keV transition to the 742.9 keV 7/2 − level being weak (cf. Fig. 10 and Table 3). The 7/2 − levels predicted at 1.07 and 1.09 MeV, if lying above the 1148.6 keV level, would therefore probably not be fed to an observable extent by direct transitions from the 2060.4 keV level. Possible 7/2 − levels could, however, be excited by transitions from Po^{207} and from higher lying 5/2 − levels. Although not quite excluded (the proposed level at 1361.0 keV might well have the spin 7/2 −), the 7/2 − levels predicted at 1.07 and 1.09 MeV seem to be weakly populated. Levels of spin values $\geqslant 9/2$ above the 992.5 keV 7/2 − level would probably not be observed from the decay of Po^{207}.

The proposed levels at 1763.1 and 1847.0 keV seem to be fed from the 2060.4

keV 3/2 + level and should accordingly have low spin values. Levels of spins 1/2 −, 3/2 − and 5/2 − due to the configuration $(f_{5/2})^{-2}h_{9/2}$ are estimated to lie at these energies. Other configurations, however, not included in Fig. 11, might also give rise to levels of low spin values.

According to the decay scheme the 1902.4, 2060.4 and 2405.6 keV levels should have even parities. Levels of even parities are estimated to lie above 1.7 MeV (cf. Fig. 11) but no detailed calculation has been made. The log ft values of about 6.5 for the electron capture to the 2060.4 and 2405.6 keV levels indicate first forbidden transitions. Levels of even parities and appropriate spins could result from the transition of a $d_{3/2}$ or a $d_{5/2}$ proton of the closed 82 proton shell into an $f_{5/2}$ neutron, filling the hole in the $f_{5/2}$ orbital, as have been suggested for the excitation of the high energy levels of Pb^{206} [3] and Pb^{205} [4]. The excitation of $i_{13/2}$ neutron states, as found in the decay of Bi^{207} [27] and in the decay of other odd Bi- and Tl-isotopes [1], might also be possible. The observed $E3$ transition from the 2060.4 keV level to the Bi^{207} ground state suggests that the first alternative be preferred. Assuming the 2060.4 and 2405.6 keV levels to be ascribed the configurations $(p_{1/2})^{-2}(h_{9/2})^2(d_{3/2})^{-1}$ and $(p_{1/2})^{-2}(h_{9/2})^2(d_{5/2})^{-1}$ with the spins 3/2 + and 5/2 + respectively, the observed 2060.8 keV $E3$ transition to the Bi^{207} ground state could be identified as the $h_{9/2} \rightarrow d_{3/2}$ proton transition and the 345.2 keV $M1$ transition between the levels could be ascribed to the $d_{5/2} \rightarrow d_{3/2}$ proton transition. It is interesting to note that the energy of the latter transition is in fair agreement with the level separation $d_{5/2} - d_{3/2}$ in odd Tl-isotopes [1].

The discussion above shows that the main features of our decay scheme are in agreement with Wahlborn's calculations. The low-lying levels may thus largely be identified with the predicted levels. In order to explain the observed transitions, however, one has to assume the presence of configuration mixing. For a more detailed comparison of the experiments with the theory improved calculations, including the effect of configuration mixing, would be desirable.

ACKNOWLEDGEMENTS

The authors are greatly indebted to Professors The Svedberg and Kai Siegbahn for their interest in this work. Thanks are due to Fil. kand. G. Bernander, who carried out part of the measurements of the conversion electron spectrum. Thanks are further due to Ing. Å. Svanheden and the synchrocyclotron crew for performing the numerous irradiations necessary for this investigation and to Miss I.-B. Svensson for aid in the preparation of spectrometer sources. The authors also wish to thank Civ. ing. S. Wahlborn for valuable discussions concerning the last chapter and for permission to include here some of his results, and Dr. P. Hillman for correcting the English.

One of us (J. B.) expresses his sincere thanks to Professor Kai Siegbahn for the hospitality which has been shown to him during his stay at the Physics Department and gratefully acknowledges a fellowship from UNESCO and a scholarship from Advocate I. Philipson family.

Part of this work has been financially supported by the Swedish Atomic Energy Commission.

The Gustaf Werner Institute for Nuclear Chemistry, and Physics Department, University of Uppsala, Uppsala, Sweden.

REFERENCES

1. I. Bergström and G. Andersson, Arkiv Fysik *12*, 415 (1957).
2. M. H. L. Pryce, Proc. Phys. Soc. *A 65*, 773 (1952).
3. D. E. Alburger and M. H. L. Pryce, Phys. Rev. *95*, 1482 (1954).
4. M. H. L. Pryce, Nuclear Physics *2*, 226 (1956/57).
5. M. J. Kearsley, Nuclear Physics *4*, 157 (1957).
6. W. W. True and K. W. Ford, Phys. Rev. (in course of publication).
7. S. Wahlborn, Nuclear Physics *3*, 644 (1957).
8. D. H. Templeton, J. J. Howland, Jr., and I. Perlman, Phys. Rev. *72*, 758 (1947).
9. A. W. Stoner, UCRL-3471, June 27, 1956 (unpublished).
10. E. Arbman and N. Svartholm, Arkiv Fysik *10*, 1 (1955).
11. P.-A. Tove, Nuclear Instr. *2*, 1 (1958).
12. T. R. Gerholm, Rev. Sci. Instr. *26*, 1069 (1955).
13. B. G. Pettersson and T. R. Gerholm, Nuclear Instr. (to be published).
14. E. Arbman, Nuclear Physics *3*, 625 (1957).
15. R. E. Bell and H. M. Skarsgard, Can. J. Phys. *34*, 745 (1956).
16. G. Rudstam and Å. Svanheden, private communication.
17. M. Mladjenović and H. Slätis, Arkiv Fysik *9*, 41 (1954).
18. R. D. Hill, E. L. Churh, and J. W. Mihelich, Rev. Sci. Instr. *23*, 523 (1952).
19. G. Bäckström, private information.
20. B. Kahn and W. S. Lyon, Nucleonics *11* (no. 11), 61 (1953).
21. M. E. Rose, G. H. Goertzel, and C. Swift, privately distributed tables.
22. L. A. Sliv and I. M. Band, privately distributed tables.
23. C. M. Davisson and R. D. Evans, Revs. Modern Phys. *24*, 79 (1952).
24. Tables for the Analysis of Beta Spectra, N.B.S. Applied Mathematics Series 13.
25. P. F. A. Klinkenberg, Revs. Modern Phys. *24*, 63 (1952).
26. I. Lindgren, Nuclear Physics (to be published).
27. D. E. Alburger and A. W. Sunyar, Phys. Rev. *99*, 695 (1955).
28. M. G. Mayer and J. H. D. Jensen, Elementary Theory of Nuclear Shell Structure, Chapter IX. John Wiley & Sons Inc., New York, 1955.
29. S. A. Moszkowski, Chapter XIII, Beta- and Gamma-Ray Spectroscopy, Ed. K. Siegbahn. North-Holland Publishing Co., Amsterdam, 1955.
30. M. Goldhaber and A. W. Sunyar, Chapter XVI (II), Beta- and Gamma-Ray Spectroscopy, Ed. K. Siegbahn. North-Holland Publishing Co., Amsterdam, 1955.
31. P. F. Zweifel, Phys. Rev. *96*, 1572 (1954).
32. S. A. Moszkowski, Phys. Rev. *82*, 35 (1951).
33. H. Brysk and M. E. Rose, ORNL-1830 (unpublished).
34. P. F. Zweifel, p. 300, Proceedings of the Rehovoth Conference on Nuclear Structure 1957, Ed. H. J. Lipkin. North-Holland Publishing Co., Amsterdam, 1958.
35. S. Wahlborn, private information.
36. R. B. Day, Phys. Rev. *102*, 767 (1956).
37. L. Cranberg and J. S. Levin, Phys. Rev. *103*, 343 (1956).
38. A. De-Shalit and M. Goldhaber, Phys. Rev. *92*, 1211 (1953).

Tryckt den 29 april 1958

Uppsala 1958. Almqvist & Wiksells Boktryckeri AB